Lanthanide-dependent isolation of phyllosphere methylotrophs selects for a phylogenetically conserved but metabolically diverse community

Alekhya M. Govindaraju[a], Colleen A. Friel[b], Nathan M. Good[a], Sidney L. Banks[a], Kenan S. Wayne[a], N. Cecilia Martinez-Gomez[#]

a. Department of Plant and Microbial Biology, University of California, Berkeley, Berkeley, CA, USA

b. Department of Microbiology and Molecular Genetics, Michigan State University, East Lansing, MI, USA

#Address correspondence to: N. Cecilia Martinez-Gomez, cecimartinez@berkeley.edu

Running Title

Lanthanide-dependent isolation of phyllosphere methylotrophs

Abstract

The influence of lanthanide biochemistry during methylotrophy demands a reassessment of how the composition and metabolic potential of methylotrophic phyllosphere communities are affected by the presence of these metals. To investigate this, methylotrophs were isolated from soybean leaves by selecting for bacteria capable of methanol oxidation with lanthanide cofactors. Of the 344 pink-pigmented facultative methylotroph isolates, none were obligately lanthanide-dependent. Phylogenetic analyses revealed that all strains were nearly identical to each other and to model strains from the *extorquens* clade of *Methylobacterium*, with *rpoB* providing higher resolution than 16s *r*RNA for strain-specific identification. Despite the low species diversity, the metabolic capabilities of the community diverged greatly. Strains encoding identical PQQ-dependent alcohol dehydrogenases displayed significantly different growth from each other on alcohols in the presence and absence of lanthanides. Several strains also lacked well-characterized lanthanide-associated genes thought to be important for phyllosphere colonization. Additionally, 3% of our isolates were capable of growth on sugars and 23% were capable of growth on aromatic acids, substantially expanding the range of multicarbon substrates utilized by members of the *extorquens* clade in the phyllosphere. Whole genome sequences of eleven novel strains are reported. Our findings suggest that the expansion of metabolic capabilities, as well as differential usage of lanthanides and their influence on metabolism among closely related strains, point to evolution of niche partitioning strategies to promote colonization of the phyllosphere.

Importance

Lanthanides are essential metals for life. The identification of lanthanide-associated processes has been well-studied in methylotrophic bacteria, which are plant symbionts that utilize reduced

one-carbon compounds for growth. Yet, the importance of lanthanides in plant-microbe interactions and the effects of lanthanides on microbial physiology and colonization in plants remains poorly understood. Here, we characterize the first methylotrophic bacterial community isolated from the phyllosphere in a lanthanide-dependent manner. We have identified strains encoding identical lanthanide-dependent enzymes yet exhibiting differences in lanthanide-associated growth, and have identified strains lacking lanthanide-associated genes thought to be important for phyllosphere colonization. In addition, we have identified many strains capable of metabolisms that were thought to be rare within this clade. Overall, our isolates serve as a microcosm by which to interrogate how lanthanides influence methylotrophic physiology in plant environments and highlights how phylogenetically similar strains can diverge greatly in metabolic potential.

Introduction

The phyllosphere, the aerial portion of plants dominated by leaves (1), is colonized by a diverse community of microorganisms (2–4). Despite the variety of potential substrates provided by plant leaves (carbohydrates, organic acids, amino acids, volatile compounds), microorganisms in the phyllosphere must overcome waxy leaf cuticles, UV light, temperature fluctuations, low water availability and other biotic and abiotic impediments to colonization (2,3). Cultivation-independent studies of the phyllosphere have only emerged within the last decade (3). A proteogenomic study characterized the phyllosphere community of *Glycine max* (soybean) and showed high levels of proteins characteristic of the *Alphaproteobacteria* class and, specifically, the *Methylobacterium* genus (5). Methylotrophs of the *Methylobacterium* genus are so-named due to their capacity to utilize reduced one-carbon compounds such as methane,

methanol, methylamine, formaldehyde, or formate as their sole source of carbon and energy (6) . In the phyllosphere, methylotrophs are well-suited to take advantage of methanol released daily by pectin methylesterases during routine plant cell wall breakdown and repair (100 Tg y^{-1}) (4,7). Methylotrophs may even stimulate plants into releasing additional methanol by secreting the plant hormone cytokinin, which triggers plant cell division (2).

In Gram-negative methylotrophic bacteria, pyrroloquinoline quinone (PQQ) methanol dehydrogenases convert methanol to formaldehyde (8). Although the first-identified methanol dehydrogenase from Gram-negative methylotrophs was the calcium (Ca^{2+}) -dependent MxaFI (6,8), recent studies have highlighted the importance of an alternative methanol dehydrogenase, XoxF, which coordinates a lanthanide atom in complex with PQQ (8–10). Prior to the discovery of XoxF, the calcium (Ca^{2+})-dependent methanol dehydrogenase MxaFI was thought to be the only enzyme responsible for methanol oxidation in this system. XoxF is widespread in the environment (11,12) and phylogenetically ancestral to MxaFI (8). Metaproteomics analysis of the soybean phyllosphere showed comparable levels of XoxF to MxaFI (5,13). In addition to XoxF, ExaF is a lanthanide-dependent alcohol dehydrogenase with sub-nanomolar K_M towards ethanol and auxiliary activity with formaldehyde, a toxic intermediate of methylotrophic metabolism (14). Induction of XoxF can repress MxaFI expression at lanthanide concentrations higher than 100 nM (15). Although the importance of lanthanide-dependent alcohol dehydrogenases in alcohol and aldehyde metabolism is clear, the extent to which lanthanides influence other metabolisms and the diverse set of proteins that regulate lanthanide-dependent processes are open areas of research.

Lanthanides have expanded our understanding of methylotrophic metabolism and ecology even beyond the phyllosphere. The addition of lanthanides to the isolation process of

93 microbial communities has led to the discovery of new cultivable methylotrophs in coal slag (16)
94 and marine environments (17), but this phenomenon has yet to be tested on phyllosphere
95 communities. Lanthanides have also unlocked previously unknown metabolic capabilities of
96 well-characterized plant symbionts. For example, a *Bradyrhizobium* strain isolated from legumes
97 displayed little to no growth on methanol, despite maintaining genes for methanol metabolism,
98 until the addition of lanthanides to the growth medium (18).
99 Lanthanide utilization during alcohol oxidation in methylotrophs has been well-
100 characterized, yet methylotrophs can also take advantage of other substrates in the phyllosphere
101 whose metabolism may or may not be influenced by lanthanides. For example, methylotrophs
102 have several mechanisms by which they can grow on the C_1 compound, methylamine.
103 Methylamine dehydrogenases (*mauFBEDACJGLMN*) catalyze the oxidation of methylamine to
104 formaldehyde, which can be further oxidized to formate for assimilation or dissimilation (6).
105 Alternatively, methylamine can be converted via the *N*-methylglutamate pathway (*mgdDCBA*,
106 *mgsABC*, *gmaS*) to methylene-tetrahydrofolate for assimilation or dissimilation, although the
107 extent of formaldehyde as an obligate intermediate in this pathway remains unknown (19). The
108 model organism *M. extorquens* AM1 encodes both pathways yet primarily uses methylamine
109 dehydrogenase during growth on methylamine, whereas the model organism *M. extorquens* PA1
110 only encodes the N-methylglutamate pathways (19,20). Organisms solely utilizing the *N*-
111 methylglutamate pathway have markedly slower growth on methylamine than those that can
112 catalyze the direct oxidation to formaldehyde (19,20).
113 *Methylobacterium* species can be further classified as pink-pigmented facultative
114 methylotrophs (PPFMs) (4) that can utilize multi-carbon substrates available in the phyllosphere,
115 including acetate (C2), pyruvate (C3), and succinate (C4). Recently, facultative methylotrophy

has expanded to include species capable of growth on sugars within the *extorquens* clade (21) and species capable of growth on methoxylated aromatic acids within the *nodulans* and *aquaticums* clades of *Methylobacterium* (22). Methylotrophic growth on the latter is predicted to occur via an initial demethoxylation of the methoxy group that is released as formaldehyde to generate protocatechuic acid; formaldehyde can be assimilated or dissimilated via methylotrophic pathways (22). The capability to utilize different carbon sources, such as methanol, ethanol, and multicarbon substrates, may explain why methylotrophs are so well-suited to life in the phyllosphere (2,5,23) where metabolite availability changes dynamically (2).

Despite extensive characterizations of the microbial community in the phyllosphere as well as recent advances in lanthanide-dependent metabolisms, the effect of lanthanides on methylotrophic community composition in the phyllosphere remains unknown. To investigate this, methylotrophs were isolated from the phyllosphere of soybean plants and selected for growth on methanol in the presence and absence of lanthanides, and then grown on different carbon substrates. Growth parameters were measured with and without the addition of lanthanum (La^{3+}). These strains were found to be phylogenetically similar but phenotypically distinct, with growth rates differentially affected by substrate identity and the presence or absence of lanthanum.

Results

The soybean phyllosphere methylotrophic community is not obligately lanthanide-dependent

Methylotrophic bacterial strains were isolated from the soybean phyllosphere by selection on minimal salts media with methanol as the sole carbon source. Previous studies have shown that the presence of lanthanides allows for the isolation of novel methylotrophic strains (16,17);

thus, we also included lanthanum in our media. Of 344 total isolates, 158 strains were isolated with the addition of La^{3+} and 186 strains without the addition of La^{3+} to the selection medium. After isolating single colonies, all 344 strains were retested for growth on methanol in the presence and absence of La^{3+} to determine if lanthanides were necessary for growth. All strains were pink, showed growth on methanol in the presence and absence of La^{3+} in the growth medium, and showed growth on succinate and were therefore all classified as PPFMs. Each strain was assigned a unique SLI (**S**oybean **L**eaf **I**solate) number, which is used to reference specific strains throughout this study (**Table 1**).

Methylotrophic communities from the soybean phyllosphere are phylogenetically similar

Chromosomal DNA was extracted from the isolates and *rpoB* regions were PCR amplified and Sanger sequenced. Using NCBI BLAST, *rpoB* sequences from each isolate were compared against the Joint Genome Institute's (JGI) Integrated Microbial Genomes (IMG) database to putatively assign species-level taxonomic classifications to each isolate. All isolates matched to *Methylobacterium* species within group B (24) , with the closest species being *Methylobacterium extorquens* AM1, *Methylobacterium extorquens* PA1, *Methylobacterium extorquens* TK001, and *Methylobacterium zatmanii* 135. Untrimmed *rpoB* sequences from each isolate, as well as from reference *Methylobacterium* and related species, were aligned using MUSCLE, and Maximum-Likelihood trees with 100 bootstrap replications were constructed using MEGA (**Figure 1A**). The *rpoB*-based trees show a high degree of relatedness amongst all isolates, integrating SLI strains among other reference methylotroph strains within the *extorquens* clade.

We sought to augment our understanding of the SLI community composition at the taxonomic level by employing pairwise average nucleotide identity (ANI) comparisons of all

orthologous genes shared among all assembled SLI genomes (see **Table 1**) and representative methylotrophic genomes using the IMG database. Results from the complete pairwise ANI comparisons can be found in the **Table S1**, but have been condensed to include only SLI strains and representative species from the *extorquens, aquaticum,* and *nodulans* clades in **Figure 1B**. Based on ANI comparisons, all SLI strains were most similar to *Methylobacterium* species from the *extorquens* clade (93-99% ANI) when compared to the *nodulans* (79% ANI) and *aquaticum* clades (78% ANI), indicating that our community likely belongs to the *extorquens* clade. Based on the 95% standard species cutoff (25), all SLI strains except for SLI 516, 575, and 576 are genetically identical to the model organisms *Methylobacterium extorquens* AM1 and PA1. Additionally, SLI 231, 233, 274, 285, 499, and 505 appear to be nearly 100% genetically identical to each other; yet, as will be discussed in detail later, they exhibit distinct metabolic differences (see **Table S2** for full comparison of genomes).

Whole-genome sequencing of representative SLI strains reveals new* extorquens *strains

The genomes of SLI strains 223, 231, 233, 274, 285, 384, 499, 505, 516, 575, 576 were sequenced through the Joint Genome Institute and annotated using the IMG Annotation Pipeline v.5.0.22. Summaries of the genome information for each strain compared to *M. extorquens* AM1 and PA1 are represented in **Table 1**. Notably, all strains but SLI 223 encoded at least one plasmid in addition to the chromosome, with most strains (SLI 231, 233, 274, 285, 499, 505, 516, 575, 576) encoding at least three additional plasmids. The size, % GC, and number of genes per chromosome and per plasmid were very similar for SLI 231, 233, 274, 285, 499, and 505 and for SLI 516, 575, 576; this underscores the high degree of ANI between the strains (**Figure 1B)**. SLI 516, 575, and 576 – which are the least similar by ANI to *M. extorquens* AM1 and PA1 (**Figure 1B**) – also have the smallest chromosome sizes despite having the broadest metabolic

capabilities (**Figure 2A**). None of the strains encoded the megaplasmid (1261460 bp) found in *M. extorquens* AM1, and the plasmid sizes of the SLI strains were very different from the plasmid sizes of *M. extorquens* AM1.

Predictions about metabolic potential can be made from genomic analysis. All genomes encode tetrahydromethanopterin and tetrahydrofolate-dependent pathways for C_1 oxidation and marker genes for the serine cycle for C_1 assimilation, indicating that all strains are Type II methylotrophs (6). All genomes encode four formate dehydrogenases, save for SLI 516, 575, and 576 which lack formate dehydrogenase 1. All genomes also encode the *N*-methylglutamate pathway for methylamine utilization (*mgdDCBA*, *mgsABC*, *gmaS*) (22,26). Strains SLI 231, 233, 274, 285, 499, 505, 516, 575, and 576 encode a previously identified gene island that confers the ability to grow on methoxylated aromatic acids (22) .

The SLI genomes can be grouped into two categories based on the presence or absence of lanthanide-associated genes: group 1 consists of SLI 223, 231, 233, 274, 285, 384, 499, 505 and group 2 consists of SLI 516, 575, and 576. Genomes from both groups encode calcium-dependent methanol dehydrogenases and cognate cytochromes (*mxaFIG*) and lanthanide-dependent methanol dehydrogenases and cognate cytochromes (*xoxFG*) indicating that all strains are capable of lanthanide-independent and lanthanide-dependent methanol metabolism. Yet, genes for the lanthanide-dependent alcohol dehydrogenase and cognate cytochrome (*exaFG*) are lacking in group 2 genomes. In addition, group 2 genomes lack the gene for the lanthanide-binding protein, lanmodulin, despite encoding the rest of the genes involved in the lanthanide utilization and transport cluster (27). Thus, the influence of lanthanides on the metabolisms of group 2 strains is of particular interest. The differences between groups 1 and 2 is also reflected

in the average nucleotide identities in **Figure 1B**. A complete summary of all metabolic and lanthanide-related genes found in the SLI strains is included in **Table S2**.

Methylotroph isolates possess broad metabolic capabilities independent of lanthanide availability

Although phyllosphere isolates were phylogenetically similar to domesticated research strains such as *M. extorquens* AM1 and PA1, we hypothesized that environmental methylotrophs might possess expanded substrate repertoires and broader metabolic capabilities. To test our hypothesis, all isolates were screened for growth on C_1 substrates (methanol, methylamine, dimethylsulfide), C_2 substrates (ethanol, oxalate), sugars (fructose, glucose), aromatic acids (vanillic acid), and complex insoluble substrates (lignin, cellulose, tyrosine) **(Table 2)**. Lanthanides were also added to growth media for each substrate, but this addition did not unlock novel substrate utilization capabilities for any SLI tested. All strains exhibited growth on methanol, methylamine, and ethanol. No strains grew on dimethylsulfide, oxalate, glucose, lignin, cellulose, or tyrosine. Notably, 10 out of 344 strains exhibited moderate to substantial growth on fructose and 78 out of 344 strains grew on vanillic acid.

The subset of SLI strains with completely sequenced genomes (SLI 223, 231, 233, 274, 285, 384, 499, 505, 516, 575, 576) that were shown to have broad metabolic capabilities from the screen described above were spotted onto solid media containing five different carbon sources without La^{3+}, with growth of *M. extorquens* PA1 serving as a comparison (**Figure 2A),** to visualize relative differences in metabolic capabilities. From this subset, all grew on methanol, confirming the initial growth phenotype, and all strains also grew on ethanol and methylamine. SLI 231, 233, 499, 505, and 575 grew on vanillic acid. Isolates that grew on vanillic acid also grew more robustly on methylamine, as evidenced by larger and more opaque colony

phenotypes. SLI 516, 575, and 576 were the only strains of this subset capable of growth on fructose. Interestingly, these three strains also exhibited biofilm formation during growth in liquid cultures (**Figure 2B, C**) and had heterogeneous colony morphology compared to all other strains (**Figure 2A**). This initial screen revealed that aromatic acid catabolism (22) and fructose utilization (21) are more widespread within the *extorquens* clade than previously assumed.

Addition of lanthanides influences the catabolism of alcohols

Based on our initial screen for substrate utilization on solid media, six representative isolates (SLI 231, 233, 384, 499, 505, 575) were chosen as a test cohort for downstream growth analyses because they displayed expanded metabolic capabilities compared to model organisms *M. extorquens* AM1 or PA1, which cannot grow on sugars or aromatic acids. To further investigate the impact of La^{3+} on this community, the growth rates and total biomass yields of the test cohort strains were compared during growth on methanol and ethanol as lanthanides have been shown to impact the oxidation of both alcohols in methylotrophic bacteria .

Growth rates (**Figure 3A, 3C**) and yields (**Figure 3B, 3D**) on 20 mM methanol and 34 mM ethanol, both with and without La^{3+} in the growth medium, were measured. Growth rates on methanol were significantly higher in the presence of La^{3+} for 5 out of 6 strains (SLI 231, SLI 233, SLI 384, SLI 499, SLI 505; **Figure 3A**). Final yields were significantly lower in the presence of La^{3+} for SLI 384 but significantly higher in the presence of La^{3+} for SLI 499 and SLI 505; thus, lanthanides can have variable effects on growth yields despite similar trends in growth rates. Even amongst nearly identical strains encoding identical lanthanide-independent and -dependent methanol dehydrogenases, there was significant variability in the final yields achieved in the presence of La^{3+} between SLI 575 and SLI 231, SLI 233, SLI 499, and SLI 505 and in the

absence of La^{3+} between SLI 233 and SLI 575 (*p*-values for significance of all strains from one-way ANOVA in **Table S3**).

Interestingly, growth rates on ethanol were higher in the presence of La^{3+} for SLI 231, SLI 233, SLI 384, SLI 499, and SLI 505 but *not* SLI 575, the only strain in the test cohort lacking ExaFG. Thus, we hypothesize that XoxFG must be acting as the primary ethanol dehydrogenase during growth on ethanol with lanthanides in this strain (14). Although SLI 231, SLI 233, SLI 384, SLI 499, and SLI 505 possess high degrees of genomic similarity (**Figure 1B**) and all strains encode identical lanthanide-dependent enzymes, SLI 384 exhibits significantly higher growth rates than the other strains in the presence of La^{3+} (*p*-values for significance of all strains from one-way ANOVA in **Table S3**). Unlike the phenotypes with methanol (**Figure 3A-B**), the presence of La^{3+} in the growth medium does not appear to have significant effects on the final yields obtained, save for SLI 505 which exhibited significantly lower yields with La^{3+}.

For most strains, the presence of La^{3+} increases growth rate in methanol but the effect on yields during growth on methanol and ethanol appear to be strain-dependent. Addition of lanthanides did not result in a universal phenotypic change during growth on alcohols despite most strains possessing nearly identical lanthanide-dependent enzymes. This raises interesting hypotheses about the differential regulation of lanthanide-dependent enzymes and metabolisms in methylotrophs and the role of lanthanide-dependent alcohol dehydrogenases during growth on ethanol specifically.

SLI strains lacking lanthanide-associated genes reveal insights into lanthanide physiology

Genomic analysis identified several genomes (SLI 516, 575, 576) that lack lanmodulin (**Table S2**) and do not have significant differences during growth on methanol or ethanol in the presence of lanthanides (**Figure 3)**. Lanmodulin is one of the most abundant proteins in the

phyllosphere (23) and can bind to lanthanides with very high affinity and selectivity (28) yet no physiological role for lanmodulin has been identified; thus, the absence of lanmodulin in a subset of SLI genomes from the phyllosphere was intriguing. To investigate the role of lanmodulin in our SLI strains, the gene *lanM* (MexAM1_META1p1786) was cloned into an IPTG-inducible expression vector and transformed into electrocompetent SLI 575. To replicate lanthanide conditions in the phyllosphere – where lanthanides can exist in soluble or poorly soluble forms at varying concentrations – lanmodulin expression was phenotyped during growth on alcohols in the presence of excess (2 µM) and limiting (50 nM) concentrations of $LaCl_3$ and La_2O_3 (**Figure 4A, B**).

SLI 575 also lacks ExaF, so ethanol oxidation in excess lanthanide conditions must be carried out by XoxF but could be facilitated by either MxaFI or XoxF in limiting lanthanide concentrations (14,15). Therefore, we hypothesized that growth phenotypes of *lanM* expression in these lanthanide conditions would be identical during growth on both methanol and ethanol. During growth on methanol, expression of *lanM* had no effect in the presence of excess soluble La^{3+} but resulted in an 8% significant decrease in growth rate with limiting soluble La^{3+} and 18-24% significant increase in growth rate with excess and limiting poorly soluble La^{3+} (**Figure 4A**). In contrast, during growth on ethanol, significant differences are only observed during growth on limiting soluble La^{3+} (8% increase) or excess poorly soluble La^{3+} (14% increase) (**Figure 4B**) . Our preliminary results indicate a putative supplementary role for lanmodulin during growth on poorly soluble lanthanide sources, but differences during growth on methanol and ethanol require further investigation.

Robust aromatic acid utilization by SLI strains reveals novel lanthanide-related phenotypes

297 Genes that confer the ability to grow on methoxylated aromatic acids (ferulic acid,
298 vanillic acid, protocatechuic acid, *p*-hydroxybenzoic acid) have been recently identified in
299 methylotrophs primarily from the *aquaticum* and *nodulans* clade (22) . These genes exist as a
300 horizontally-transferred genetic island that is notably absent from the *extorquens* clade, save for
301 their presence in *Methylobacterium sp.* AMS5 (22) . Our screen isolated 78 strains capable of
302 growth on the methoxylated aromatic acid, vanillic acid. Of the SLI strains with assembled
303 genomes, those capable of growth on vanillic acid encode gene islands identical to each other
304 (**Table S2**). Aromatic acid gene islands in SLI strains include all of the genes found in the
305 aromatic acid gene island in *Methylobacterium sp.* AMS5 although specific regulatory genes are
306 in a different order. To demonstrate the robustness of SLI growth on aromatic acids, SLI strains
307 from the test cohort were grown on a low (5 mM) and high (12 mM) concentration of vanillic
308 acid (22,29,30) in the presence and absence of $LaCl_3$ and their growth was compared to that of
309 *Methylobacterium sp.* AMS5 (**Figure 5**). SLI 384 was used as a control, as it does not encode
310 genes for vanillic acid catabolism and therefore does not grow on vanillic acid (**Figure 2**).
311 Two striking phenotypes emerge when comparing growth on different concentrations of
312 vanillic acid. First, all strains exhibit slower growth rates on high concentrations of vanillic acid
313 compared to low concentrations of vanillic acid (**Figure 5A, C**). Despite encoding nearly
314 identical aromatic acid gene islands, *Methylobacterium sp.* AMS5 exhibits poor growth on high
315 concentrations of vanillic acid compared to the SLI strains (**Figure 5C)** and there are significant
316 differences in growth between the SLI strains as well (p-values for significance of all strains
317 from one-way ANOVA in **Table S3**). Second, addition of lanthanides influences aromatic acid
318 utilization based on substrate concentration despite all SLI strains encoding identical aromatic
319 acid gene islands. SLI 505 has higher growth rates with lanthanides on 5 mM vanillic acid but

lower growth rates with lanthanides on 12 mM vanillic acid (**Figure 5A, C)**. SLI 231 has lower growth rates with lanthanides only during growth on 12 mM vanillic acid, a trend also seen in SLI 499 although the differences are not significant (**Figure 5C**). Conversely, SLI 233 has marginally higher growth rates during growth on 12 mM vanillic acid **(Figure 5C**). Lanthanides variably affect final yields during growth on low concentrations of vanillic acid (**Figure 5B**), but have little effect on yield during growth on high concentrations of vanillic acid (**Figure 5D**).

SLI strains encode identical methylamine oxidation genes but display different growth phenotypes

All SLI genomes only encode genes for the *N*-methylglutamate pathway similar to what is found in *M. extorquens* PA1 for methylamine utilization (19). To determine if the growth of SLI strains on methylamine is influenced by lanthanides, SLI strains were grown in 15 mM methylamine in the presence and absence of $LaCl_3$. Growth rates (**Figure 6A**) and final yields (**Figure 6B**) are reported. Addition of $LaCl_3$ did not significantly impact the growth rate or yield for any strain tested. Interestingly, SLI 575 had significantly lower yields than SLI 231, 233, 499, and 509, despite having a similar growth rate to all four strains; this trend was not lanthanide-dependent. Also of note, SLI 384 had nearly triple the lag time and half the growth rate and final yield as other SLI strains despite encoding identical *N*-methylglutamate pathway genes. This suggests additional details about methylamine catabolism in SLI strains beyond the *N*-methylglutamate pathway that result in the diminished growth phenotypes observed.

SLI strains expand fructose utilization in the extorquens clade

Most methylotrophs, including *M. extorquens* AM1 and PA1, encode all of the genes necessary for sugar oxidation but lack sugar-specific transporters and assimilatory pathways required for their utilization as a primary substrate (26). Notably, complete sugar catabolism has

only been demonstrated in endophytic *extorquens* clade members (21). Thus, it was striking to isolate ten strains capable of robust growth on fructose as the sole carbon source (**Table 2**). Of the strains with assembled genomes, SLI 516, SLI 575, and SLI 576 were capable of growth on fructose. Interestingly, these three SLI strains also displayed the lowest sequence similarity to other SLI strains and to *M. extorquens* AM1 and PA1 based on ANI (**Figure 1B**), hinting that the differences in genomes might be due in part to unknown genes specific to sugar transport and catabolism. To quantify growth on fructose, SLI 575 was grown on 25 mM fructose in the presence and absence of $LaCl_3$ (**Figure 7**). Growth rates and yields in both conditions were nearly identical. Growth rates on fructose were comparable to rates for methylamine and substantially lower than rates for methanol or vanillic acid. To our knowledge, SLI 516, 575, and 576 are the first identified epiphytic *extorquens* strains capable of growth on a sugar substrate.

Discussion

Methylotrophs that inhabit the phyllosphere influence both the plants that they colonize and global biogeochemical processes (1,4). Yet, studies investigating the physiology, biodiversity, and ecology of methylotrophic communities of the phyllosphere have only emerged within the last decade (3,31) and do not take into account the role of lanthanides in influencing their community composition. Furthermore, despite the abundance of methylotrophs in the phyllosphere, the bulk of phylogenomic studies on *Methylobacterium* species use genomes isolated from non-phyllosphere environments (24). Here, we describe the first community-level characterization of the role of lanthanides during the metabolisms of natural methylotrophic populations in soybean plants, revealing novel insights into methylotrophic biodiversity, metabolic capabilities, and lanthanide-dependent metabolisms.

Marker gene sequencing for assigning taxonomic groups has proven difficult in *Methylobacterium*, as16s *r*RNA has poor phylogenetic resolution in *Methylobacterium* (24). We characterized our soybean methylotroph community composition using *rpoB* (**Figure 1A**), a highly polymorphic single-copy gene with sub-species resolution with *Methylobacterium* (24). Our phylogenetic analysis revealed two insights: 1) all of our isolates are closely related to each other (**Figure 1A**) and fall within the *extorquens* clade of *Methylobacterium* (**Figure 1A, B**), and 2) even amongst nearly identical strains (**Figure 1B**), there is broad diversity in terms of the possession of lanthanide-related genes and metabolic capabilities, and that these differences are reflected in how strains group based on *rpoB* sequences (**Figure 8**). Overall, our results substantiate *rpoB* as a superior marker gene for phylogenetic analysis of *Methylobacterium* species, and, importantly, highlight how phenotypic characterizations can reveal novel strains that appear identical by *rpoB* sequence alone.

Crops, such as soybeans, can sequester lanthanides from the soil through repeated cycles of harvest limiting lanthanide availability in the soil and affecting lanthanide availability for methylotrophs in the phyllosphere. Thus, it is not surprising that our microbial isolation from soybean plants did not reveal any novel lanthanide-dependent phenotypes despite previous studies identifying organisms that have increased heterogeneity in the presence of lanthanides (32) or that are strictly dependent on lanthanides for growth (17,18). The maintenance of both calcium-dependent and lanthanide-dependent methanol dehydrogenase systems in our SLI strains could suggest that 1) lanthanides are not always present or bioavailable in the phyllosphere and therefore MxaFI remains essential for methylotrophic growth; 2) lanthanides are present but extensively competed for, so calcium-dependent methanol oxidation systems offer an alternative for methylotrophic growth; and/or 3) lanthanide-dependent enzymes have

388 additional non-metabolic or non-lanthanide-related functions that necessitate their maintenance.
389 These hypotheses could be examined further by repeating our isolations in non-domesticated
390 phyllosphere environments where lanthanides are more prevalent or bioavailable and where the
391 isolation of obligately lanthanide-dependent methylotrophs might be more likely.

392 Notably, of the test cohort reported here, SLI 575 does not encode ExaF or lanmodulin
393 and is the only strain that does not exhibit significant lanthanide-dependent growth phenotypes
394 on alcohols (**Figure 3**). As lanmodulin is reported to be one of the most highly expressed
395 peptides in the phyllosphere (23), has been proposed to function as a lanthanide biosensor, and
396 has been shown to bind lanthanides (28) it is possible that SLI 575 is lacking the sensor required
397 to coordinate lanthanide availability with metabolic processes and the role of lanmodulin in the
398 phyllosphere specifically remains unknown. A previous study in *Methylobacterium aquaticum*
399 22A, which natively encodes *lanM*, found that overexpression of *lanM* results in faster growth on
400 methanol with 20 nM $LaCl_3$ and slower growth with 100 nM $LaCl_3$ (33). In our SLI strain
401 lacking lanmodulin, we see a similar trend during growth on methanol where *lanM* expression *in*
402 *trans* decreases growth rates at higher lanthanide concentrations but increases growth rates at
403 lower lanthanide concentrations. However, our results using poorly soluble lanthanide
404 concentrations and ethanol as a substrate are novel, and additional experiments involving ICP-
405 MS are required to determine the effect of lanmodulin mutants on intracellular lanthanide
406 concentrations. Here, SLI 575 and related strains (SLI 516, 576) emerge as an interesting model
407 by which to interrogate the role of ExaF or lanmodulin in methylotrophs both in laboratory and
408 plant environments.

409 Previous studies have reported that the model organism *M. extorquens* PA1 has an
410 average growth rate of 0.042 h^{-1} and an average final yield of OD_{600} 0.712 on 15 mM

411 methylamine (19,20). While our SLI strains exhibit similar growth rates regardless of $LaCl_3$
412 addition (**Figure 6A**), the final yields are nearly half of what is achieved by PA1 (**Figure 6B**);
413 this suggests metabolic bottlenecks towards efficient methylamine assimilation that are not
414 immediately obvious from a preliminary genomic analysis of C1 assimilation genes. One
415 possibility is that methylamine that is incorporated via the N-methylglutamate pathway
416 preferentially serves as a nitrogen source rather than a carbon source (19,20) but future studies
417 are required to validate this hypothesis in our SLI strains.
418 Although the ability to utilize methanol as a substrate has provided a competitive
419 advantage for methylotrophs in the phyllosphere, sugars and aromatic acid are abundant enough
420 to support the growth of diverse microorganisms (2,22,34). It is therefore advantageous for
421 microbes to be able to utilize both multicarbon sources, such as fructose and vanillic acid, and
422 single carbon sources like methanol. Detailed investigations into methylotrophic aromatic acid
423 catabolism in the presence and absence of lanthanides is necessary to understand how this
424 metabolism functions in carbon cycling of lignin by-products in natural environments, as well as
425 identify additional roles for lanthanides in the metabolism of non-alcohol substrates. The
426 decrease in growth rates in the presence of lanthanides only during growth on high
427 concentrations of aromatic acid is surprising, considering that all known lanthanide-dependent
428 enzymes are in the periplasm yet all enzymes used for aromatic acid utilization are in the
429 cytoplasm; the role of lanthanides during this metabolism is an ongoing area of research. The
430 substantial yield but decreased growth rate achieved by SLI strains on high concentrations vs low
431 concentrations of vanillic acid demonstrates that the ability to grow on methoxylated aromatic
432 acids is widely distributed among members of the *extorquens* clade, more robust than what has

been reported in other model strains, and could reveal novel insights about lanthanide metabolism.

Genomic analyses for fructose transporters or assimilatory pathways in SLI 516, 575, or 576 (SLI strains with assembled genomes capable of growth on fructose) identified genes encoding for phosphofructokinase that were absent in all other SLI strains. Phosphofructokinase is a key regulatory enzyme of glycolysis, responsible for the phosphorylation of fructose to fructose-6-phosphate. The end-product of this reaction is also an intermediate of the assimilatory RuMP cycle; however, none of our SLI strains employ the RuMP cycle for assimilation.

Taken together, the methylotrophic community in the phyllosphere of soybeans is metabolically diverse and heavily influenced by lanthanide availability when consuming methanol. We hypothesize that the capacity to expand substrate repertoires might also be important drivers of efficient colonization. Whether the selection for low species diversity is at the level of the plant or arises through natural selection within methylotrophic communities, this finding points to the evolution of niche partitioning strategies among a single species in order to maximize resources in shared habitats (31,35,36). Results from this study pave the way for future work to investigate 1) expanded metabolic capabilities in *extorquens* clade methylotrophs, 2) tradeoffs associated with lanthanide-dependent and -independent alcohol metabolism, and 3) niche partitioning among genetically identical strains during plant colonization.

Materials & Methods

Methylotroph isolation

Environmental methylotrophic bacterial strains were isolated from soybean plants (*Glycine max*) growing on the Michigan State University Agronomy Farm (East Lansing,

Michigan, U.S.A. 42.6908, -84.4866). Four leaves were harvested from four different plants on September 7, 2018, and each leaf was placed into a sterile 50 mL conical tube. 50 ml of sterile 50 mM phosphate buffer (pH 7.3) was added to each tube, the tubes were vortexed for 5 minutes, and 100 µL of buffer was spread onto solidified (1.5% wt/vol agar) MP minimal salts media (37). The isolation medium contained 125 mM methanol, RPMI 1640 Vitamins Solution (Sigma Aldrich, St. Louis, MO, USA) diluted to 1X, and 50 µg/mL cycloheximide. Two sets of isolation media were prepared; one with and one without 2 µM $LaCl_3$. Isolation plates were grown at 30 °C for several days until bacterial colonies were visible. Pink colonies were selected from the plates and struck out for isolated colonies onto solidified media of the same composition to confirm growth. Single colonies of isolated strains were then inoculated into 650 µL of MP medium with 125 mM methanol and 1X RPMI 1640 Vitamins Solution in a 48 well microplate. All isolated strains were inoculated into medium with the same concentration of La^{3+} as they were isolated with, and then incubated shaking for 48 hours at 200 rpm on an Innova 2300 platform shaker (Eppendorf, Hamburg, Germany) at 30°C. Strains were frozen for future use by adding 25 µL of sterile dimethyl sulfoxide to 500 µL of late-exponential phase culture in a sterile screw-cap vial, flash-freezing in liquid nitrogen, and storing at -80°C.

Strains cultivation

Cultures used for growing and maintaining strains, extracting DNA, and subculturing for growth phenotypic analyses were prepared as follows: Freezer stocks of each strain were struck out onto MP agar supplemented with 15 mM succinate and 1X RPMI 1640 Vitamins Solution and incubated at 30°C until single colonies emerged (2-4 days). Single colonies of each strain were used to inoculate 3 mL cultures of MP with 15 mM succinate and 1X RPMI 1640 Vitamins Solution and grown overnight in round-bottom glass culture tubes (ThermoFisher Scientific,

Waltham, MA, USA) at 30°C, shaking at 200 rpm on an Innova S44i shaker (Eppendorf, Hamburg, Germany) to an OD_{600} of approximately 1.5. See sections below for downstream analyses performed on these cultures.

Chromosomal DNA extraction for whole-genome and marker gene sequencing

Genomic DNA was extracted from 3 mL overnight cultures of each strain (see ***Strains Cultivation***) using the DNeasy PowerSoil Pro Kit from Qiagen (Hilden, Germany) per manufacturer's protocol. Genomic DNA was quantified using a Take3 Microvolume Plate Spectrophotometer (BioTek, Winooski, VT, USA). Whole-genome sequencing via PacBio Sequel II was performed by the Department of Energy's Joint Genome Institute (JGI, Walnut Creek, CA, USA). Genomes can be accessed through JGI Integrated Microbial Genomes & Microbiomes (IMG) (see **Table 1** for IMG Genome IDs). Marker gene sequencing was performed by PCR amplifying regions of *16s* rRNA or *rpoB* using universal primers[18] (16s_fwd: 5'GAGTTTGATCCTGGCTCA3', 16s_rev: 5'TACCTTGTTACGACTT3'; rpoB_fwd: 5'AAGGACATCAAGGAGCAGGA3', rpoB_rev: 5'ACSCGGTAKATGTCGAACAG3'), confirming products via gel electrophoresis on a 1% agarose gel, purifying PCR products using the GeneJET PCR Purification Kit (ThermoFisher Scientific, Waltham, MA, USA) , and Sanger sequencing the PCR products. Untrimmed sequences were aligned using MAFFT and MUSCLE, and a Maximum-Likelihood tree using a Tamura-Nei model and 100 bootstrap replications was constructed using MEGA. Average nucleotide identity scores were calculated through JGI IMG interface for pairwise genome comparisons using whole-genome sequences from the IMG database as inputs.

Growth phenotypic analyses

Isolate strains were cultivated as described in ***Strains Cultivation*** and were screened for their ability to grow on diverse substrates in the presence and absence of La^{3+}. To screen for the ability to grow on diverse substrates, overnight cultures of each strain were washed twice in MP media with no carbon source at 2000 x g for 10 minutes, resuspended in MP media to an OD600 of 0.1, and spotted (10 uL) onto MP agar plates supplemented with 1X 1640 RPMI Vitamins Solution, and either a soluble substrate (20 mM methanol, 34 mM ethanol, 15 mM methylamine, 5 mM potassium oxalate, 25 mM glucose, 25 mM fructose) or an insoluble substrate (5 mM vanillic acid); the insoluble substrates were added as non-sterilized powders directly to the melted agar prior to pouring the plate. Agar plates were incubated at 30C for 2-4 days or until visible colonies formed.

To screen for La^{3+} effects during growth on methanol, overnight cultures of each strain were washed twice in MP media with no carbon source at 2000 x g for 10 minutes and inoculated at an OD600 of 0.1 into a transparent 96-well plate (Corning, Corning, NY, USA) containing 200 uL of MP media supplemented with 125 mM methanol, 1X RPMI 1640 Vitamins Solution, and +/- 2 μM $LaCl_3$ for endpoint growth assays. Strains with demonstrated growth on solid media of different substrates were additionally phenotyped in liquid media in the presence and absence of La^{3+}. Overnight cultures of strains of interest were washed twice in MP media with no carbon source at 2000 x g for 10 minutes and inoculated at an OD600 of 0.1 into a transparent 48-well plate (Corning, Corning, NY, USA) containing 650 uL of MP media supplemented with 1X 1640 RPMI Vitamins Solution, +/- 2 μM $LaCl_3$, and appropriate carbon source (20 mM methanol, 15 mM methylamine, 34 mM ethanol, 12 mM vanillic acid, 25 mM fructose). All endpoint assays and growth curves were carried out at 30°C and 548 rpm using a Synergy HTX plate reader (BioTek, Winooski, VT, USA) with OD600 readings measured every

30 minutes. Data was analyzed using Microsoft Excel. 2-4 replicates were run for each strain in each condition, and at least 10 exponential-phase data points were used for linear regression analysis to calculate the growth rates of each strain. Paired t-tests were performed to identify statistically significant ($p < 0.05$) differences between growth in the presence or absence of $LaCl_3$ for each strain. One-way ANOVA with post-hoc Tukey HSD was performed to identify statistically significant ($p < 0.05$) differences among all strains in the presence or absence of $LaCl_3$..

Design and construction of lanM expression vector

The expression vector encoding the IPTG-inducible promoter $P_{L/04/A1}$ and mCherry (38) was modified to include the ribosome binding site (agggagagaccccga) for *fae* (MexAM1_META1p1766) and a KpnI cut site between the XbaI and HindIII cut sites natively on the plasmid. Briefly, complementary single-stranded oligos were synthesized encoding an XbaI cut site, the entire sequence of the ribosome binding site, KpnI cut site sequence, and HindIII cut site sequence. Oligos were annealed to each other to generate a double-stranded DNA fragment, which underwent a restriction enzyme digest with XbaI (New England Biolabs, Ipswich, MT, USA) and HindIII (New England Biolabs, Ipswich, MT, USA) at 37°C for one hour. The expression vector was also digested with XbaI and HindIII under the same conditions to remove the gene for mCherry. The digested DNA fragment and vector were ligated using T4 DNA ligase (New England Biolabs, Ipswich, MA, USA) at room temperature for 10 minutes and electroporated into 10β *E. coli* competent cells (New England Biolabs, Ipswich, MA, USA). Modified plasmids encoding a ribosome-binding site were verified by colony PCR and full plasmid sequencing (Primordium Labs, South San Francisco, CA, USA). The gene for

lanmodulin (*lanM,* MexAM1_META1p1786) was amplified by PCR with primers including regions overlapping the expression vector between the ribosome-binding site and HindIII site. The expression vector was linearized by PCR with primers including regions overlapping with 20 bp of the start and end of *lanM* and treated with DpnI at 37°C for one hour. NEBuilder HiFi DNA Assembly (New England Biolabs, Ipswich, MA, USA) was used per manufacturer's protocols to assemble the expression plasmid encoding *lanM*. The assembly was electroporated into 10β *E. coli* competent cells (New England Biolabs, Ipswich, MA, USA) . The *lanM* expression vector was verified by colony PCR and full plasmid sequencing (Primordium Labs, South San Francisco, CA, USA) and electroporated into SLI 575 at 2500 V with an outgrowth in Nutrient Broth for approximately 12 hours, and SLI 575 containing the *lanM* expression vector was selected for on minimal media plates supplemented with succinate and 50 µg/mL kanamycin. All growth experiments with SLI 575/ *lanM* were carried out in media supplemented with 50 µg/mL kanamycin and, if induced, 1 mM IPTG.

Acknowledgements

We thank Allison Hunt and Zachary Jensen—previous members of the Martinez-Gomez Lab—for their invaluable efforts during the early stages of this project. We thank members of Tobias Erb's lab at the Max Planck Institute for Terrestrial Microbiology for generously providing an IPTG-inducible expression vector. We would also like to acknowledge Jean-Baptiste Leducq, Christopher Marx, Alexander Alleman, and all members of the Marx Lab at the University of Idaho for their thoughtful comments and suggestions during experimental planning and manuscript drafting. The information, data, or work presented herein was funded by the United States Department of Energy, Office of Science, Office of Biological and Environmental

Research, under Award Number DE-SC0022318 subaward SH5849-772894; by the National Science Foundation under Grant 2142154; by the National Science Foundation under Grant 2127732. A.G. was supported in part by the National Institutes of Health Genetic Dissection of Cells and Organisms Training Grant 1T32GM132022-01.

Competing Interests

The authors declare no competing financial interests.

Data Availability

The data generated and/or analyzed during the current study as well as stocks of novel reported strains are available from the corresponding author upon reasonable request. Genomes from novel strains reported in this study can be found through JGI IMG using the IMG Genome IDs indicated in **Table 1**.

References

1. Vacher C, Hampe A, Porté AJ, Sauer U, Compant S, Morris CE. The Phyllosphere: Microbial Jungle at the Plant–Climate Interface. Annu Rev Ecol Evol Syst. 2016 Nov 1;47(1):1–24.
2. Lindow SE, Brandl MT. Microbiology of the phyllosphere. Appl Environ Microbiol. 2003 Apr;69(4):1875–83.
3. Vorholt JA. Microbial life in the phyllosphere. Nat Rev Microbiol. 2012 Dec 1;10(12):828–40.
4. Yurimoto H, Shiraishi K, Sakai Y. Physiology of Methylotrophs Living in the Phyllosphere. Microorganisms. 2021;9(4).

5. Delmotte N, Knief C, Chaffron S, Innerebner G, Roschitzki B, Schlapbach R, et al. Community proteogenomics reveals insights into the physiology of phyllosphere bacteria. Proc Natl Acad Sci. 2009;106(38):16428–33.

6. Chistoserdova L, Lidstrom ME. Aerobic Methylotrophic Prokaryotes. In: Rosenberg E, DeLong EF, Lory S, Stackebrandt E, Thompson F, editors. The Prokaryotes: Prokaryotic Physiology and Biochemistry [Internet]. Berlin, Heidelberg: Springer Berlin Heidelberg; 2013. p. 267–85. Available from: https://doi.org/10.1007/978-3-642-30141-4_68

7. Galbally IE, Kirstine W. The Production of Methanol by Flowering Plants and the Global Cycle of Methanol. J Atmospheric Chem. 2002 Nov 1;43(3):195–229.

8. Keltjens JT, Pol A, Reimann J, Op den Camp HJM. PQQ-dependent methanol dehydrogenases: rare-earth elements make a difference. Appl Microbiol Biotechnol. 2014 Jul 1;98(14):6163–83.

9. Good NM, Moore RS, Suriano CJ, Martinez-Gomez NC. Contrasting in vitro and in vivo methanol oxidation activities of lanthanide-dependent alcohol dehydrogenases XoxF1 and ExaF from *Methylobacterium extorquens AM1*. Sci Rep. 2019 Mar 12;9(1):4248.

10. Nakagawa T, Mitsui R, Tani A, Sasa K, Tashiro S, Iwama T, et al. A Catalytic Role of XoxF1 as La3+-Dependent Methanol Dehydrogenase in *Methylobacterium extorquens* Strain AM1. PLOS ONE. 2012 Nov 27;7(11):e50480.

11. Huang J, Yu Z, Groom J, Cheng JF, Tarver A, Yoshikuni Y, et al. Rare earth element alcohol dehydrogenases widely occur among globally distributed, numerically abundant and environmentally important microbes. ISME J. 2019 Aug 1;13(8):2005–17.

12. Taubert M, Grob C, Howat AM, Burns OJ, Dixon JL, Chen Y, et al. XoxF encoding an alternative methanol dehydrogenase is widespread in coastal marine environments. Environ Microbiol. 2015 Oct;17(10):3937–48.

13. Knief C, Delmotte N, Chaffron S, Stark M, Innerebner G, Wassmann R, et al. Metaproteogenomic analysis of microbial communities in the phyllosphere and rhizosphere of rice. ISME J. 2012 Jul 1;6(7):1378–90.

14. Good NM, Vu HN, Suriano CJ, Subuyuj GA, Skovran E, Martinez-Gomez NC. Pyrroloquinoline Quinone Ethanol Dehydrogenase in *Methylobacterium extorquens* AM1 Extends Lanthanide-Dependent Metabolism to Multicarbon Substrates. J Bacteriol. 2016 Nov 15;198(22):3109–18.

15. Vu Huong N., Subuyuj Gabriel A., Vijayakumar Srividhya, Good Nathan M., Martinez-Gomez N. Cecilia, Skovran Elizabeth. Lanthanide-Dependent Regulation of Methanol Oxidation Systems in *Methylobacterium extorquens* AM1 and Their Contribution to Methanol Growth. J Bacteriol. 2016 Mar 31;198(8):1250–9.

16. Wegner Carl-Eric, Gorniak Linda, Riedel Stefan, Westermann Martin, Küsel Kirsten. Lanthanide-Dependent Methylotrophs of the Family Beijerinckiaceae: Physiological and Genomic Insights. Appl Environ Microbiol. 2019 Dec 13;86(1):e01830-19.

17. Howat AM, Vollmers J, Taubert M, Grob C, Dixon JL, Todd JD, et al. Comparative Genomics and Mutational Analysis Reveals a Novel XoxF-Utilizing Methylotroph in the Roseobacter Group Isolated From the Marine Environment. Front Microbiol [Internet]. 2018;9. Available from: https://www.frontiersin.org/articles/10.3389/fmicb.2018.00766

18. Wang L, Suganuma S, Hibino A, Mitsui R, Tani A, Matsumoto T, et al. Lanthanide-dependent methanol dehydrogenase from the legume symbiotic nitrogen-fixing bacterium *Bradyrhizobium diazoefficiens* strain USDA110. Enzyme Microb Technol. 2019 Nov;130:109371.

19. Nayak DD, Marx CJ. Methylamine utilization via the N-methylglutamate pathway in *Methylobacterium extorquens* PA1 involves a novel flow of carbon through C1 assimilation and dissimilation pathways. J Bacteriol. 2014 Dec;196(23):4130–9.

639 20. Nayak DD, Marx CJ. Experimental Horizontal Gene Transfer of Methylamine Dehydrogenase
640 Mimics Prevalent Exchange in Nature and Overcomes the Methylamine Growth
641 Constraints Posed by the Sub-Optimal N-Methylglutamate Pathway. Microorganisms. 2015 Mar
642 10;3(1):60–79.
643 21. Van Aken B, Peres CM, Doty SL, Yoon JM, Schnoor JL. *Methylobacterium populi* sp. nov., a
644 novel aerobic, pink-pigmented, facultatively methylotrophic, methane-utilizing bacterium isolated
645 from poplar trees (Populus deltoides×nigra DN34). Vol. 54, International Journal of Systematic
646 and Evolutionary Microbiology,. Microbiology Society,; 2004. p. 1191–6.
647 22. Lee JA, Stolyar S, Marx CJ. Aerobic Methoxydotrophy: Growth on Methoxylated Aromatic
648 Compounds by Methylobacteriaceae. Front Microbiol [Internet]. 2022;13. Available from:
649 https://www.frontiersin.org/article/10.3389/fmicb.2022.849573
650 23. Ochsner AM, Hemmerle L, Vonderach T, Nüssli R, Bortfeld-Miller M, Hattendorf B, et al. Use
651 of rare-earth elements in the phyllosphere colonizer *Methylobacterium extorquens* PA1. Mol
652 Microbiol. 2019 May 1;111(5):1152–66.
653 24. Leducq JB, Sneddon D, Santos M, Condrain-Morel D, Bourret G, Martinez-Gomez NC, et al.
654 Comprehensive Phylogenomics of *Methylobacterium* Reveals Four Evolutionary Distinct Groups
655 and Underappreciated Phyllosphere Diversity. Genome Biol Evol. 2022 Aug 3;14(8).
656 25. Figueras MJ, Beaz-Hidalgo R, Hossain MJ, Liles MR. Taxonomic affiliation of new genomes
657 should be verified using average nucleotide identity and multilocus phylogenetic analysis. Genome
658 Announc. 2014 Dec 4;2(6).
659 26. Chistoserdova L, Kalyuzhnaya MG, Lidstrom ME. The expanding world of methylotrophic
660 metabolism. Annu Rev Microbiol. 2009;63:477–99.

27. Roszczenko-Jasińska P, Vu HN, Subuyuj GA, Crisostomo RV, Cai J, Lien NF, et al. Gene products and processes contributing to lanthanide homeostasis and methanol metabolism in *Methylorubrum extorquens* AM1. Sci Rep. 2020 Jul 29;10(1):12663.

28. Cotruvo JA Jr, Featherston ER, Mattocks JA, Ho JV, Laremore TN. Lanmodulin: A Highly Selective Lanthanide-Binding Protein from a Lanthanide-Utilizing Bacterium. J Am Chem Soc. 2018 Nov 7;140(44):15056–61.

29. Varman AM, He L, Follenfant R, Wu W, Wemmer S, Wrobel SA, et al. Decoding how a soil bacterium extracts building blocks and metabolic energy from ligninolysis provides road map for lignin valorization. Proc Natl Acad Sci. 2016 Oct 4;113(40):E5802.

30. Kamimura N, Takahashi K, Mori K, Araki T, Fujita M, Higuchi Y, et al. Bacterial catabolism of lignin-derived aromatics: New findings in a recent decade: Update on bacterial lignin catabolism. Environ Microbiol Rep. 2017 Dec 1;9(6):679–705.

31. Schäfer M, Vogel CM, Bortfeld-Miller M, Mittelviefhaus M, Vorholt JA. Mapping phyllosphere microbiota interactions in planta to establish genotype–phenotype relationships. Nat Microbiol. 2022 Jun 1;7(6):856–67.

32. Skovran E, Martinez-Gomez NC. Just add lanthanides. Science. 2015 May 22;348(6237):862–3.

33. Fujitani Y, Shibata T, Tani A. A Periplasmic Lanthanide Mediator, Lanmodulin, in *Methylobacterium aquaticum* Strain 22A. Front Microbiol [Internet]. 2022;13. Available from: https://www.frontiersin.org/articles/10.3389/fmicb.2022.921636

34. Welte CU, de Graaf R, Dalcin Martins P, Jansen RS, Jetten MSM, Kurth JM. A novel methoxydotrophic metabolism discovered in the hyperthermophilic archaeon *Archaeoglobus fulgidus*. Environ Microbiol. 2021 Jul 1;23(7):4017–33.

683 35. Schlechter RO, Kear EJ, Bernach M, Remus DM, Remus-Emsermann MNP. Metabolic resource
684 overlap impacts competition among phyllosphere bacteria. ISME J. 2023 Sep 1;17(9):1445–54.
685 36. Schäfer M, Pacheco AR, Künzler R, Bortfeld-Miller M, Field CM, Vayena E, et al. Metabolic
686 interaction models recapitulate leaf microbiota ecology. Science. 381(6653):eadf5121.
687 37. Delaney NF, Kaczmarek ME, Ward LM, Swanson PK, Lee MC, Marx CJ. Development of an
688 Optimized Medium, Strain and High-Throughput Culturing Methods for *Methylobacterium*
689 *extorquens*. PLOS ONE. 2013 Apr 30;8(4):e62957.
690 38. Carrillo M, Wagner M, Petit F, Dransfeld A, Becker A, Erb TJ. Design and Control of
691 Extrachromosomal Elements in *Methylorubrum extorquens* AM1. ACS Synth Biol. 2019 Nov
692 15;8(11):2451–6.
693
694
695

696 **Table 1.** Summary of SLI strain genomes. Whole-genome sequencing performed by Joint

697 Genome Institute and annotations obtained using IMG Annotation Pipeline v.5.0.22

Strain Information			Chromosome			Plasmid		
Strain	**Proposed Name**	**IMG Genome ID**	**Size (bp)**	**% GC**	**No. of genes**	**Size (bp)**	**% GC**	**No. of genes**
M. extorquens AM1	-	644736386	5511322	68.71	5029	1261460 44195 37858 24943	67.65 67.93 65.25 66.94	1168 33 34 30
M. extorquens PA1	-	641228497	5471154	68.18	4939	-	-	-
SLI 223	*M. extorquens* SLI 223	2917523761	5504362	68.23	5222	-	-	-
SLI 231	*M. extorquens* SLI 231	2918956041	5373034	68.29	5165	166358 27292 29644	67.47 61.51 58.78	176 25 27
SLI 233	*M. extorquens* SLI 233	2932223180	5373474	68.29	5287	166399 27296 29645	67.47 61.51 58.79	181 28 27
SLI 274	*M. extorquens* SLI 274	2947147188	5374052	68.29	5202	166386 27292 29646	67.47 61.51 58.79	178 26 27
SLI 285	*M. extorquens* SLI 285	2932228704	5375017	68.30	5295	166399 27292 29655	67.47 61.51 58.78	182 25 28
SLI 384	*M. extorquens* SLI 384	2918961435	5504365	68.23	5233	28462	67.45	48
SLI 499	*M. extorquens* SLI 499	2947152626	5373409	68.29	5218	166383 27292 29645	67.47 61.51 58.79	178 25 27
SLI 505	*M. extorquens* SLI 505	2918966707	5372985	68.29	5170	166379 27292 29645	67.47 61.51 58.79	176 26 27
SLI 516	*M. extorquens* SLI 516	2918972107	5009907	68.66	4762	199519 28884 20194	67.26 66.85 60.93	215 39 30
SLI 575	*M. extorquens* SLI 575	2918977154	5009893	68.66	4764	199519 28890 20194	67.26 66.84 60.93	214 39 30
SLI 576	*M. extorquens* SLI 576	2918982202	5009856	68.66	4762	199518 28890 20194	67.26 66.84 60.93	215 39 31

A

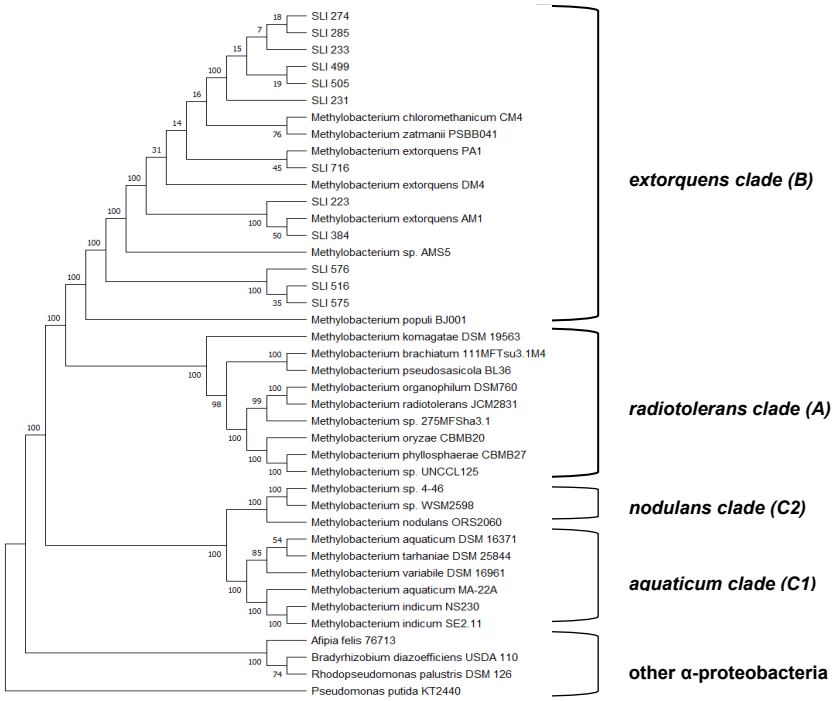

B

	Methylobacterium aquaticum MA-22A	Methylobacterium extorquens AM1	Methylobacterium extorquens PA1	Methylobacterium nodulans ORS 2060	SLI 223	SLI 231	SLI 233	SLI 274	SLI 285	SLI 384	SLI 499	SLI 505	SLI 516	SLI 575	SLI 576	SLI 716
Methylobacterium aquaticum MA-22A	100.0	79.5	79.3	82.5	79.3	79.4	79.4	79.4	79.4	79.3	79.4	79.4	79.2	79.2	79.2	79.3
Methylobacterium extorquens AM1	79.4	100.0	97.3	78.8	99.8	97.4	97.3	97.4	97.4	99.8	97.4	97.4	93.3	93.3	93.3	97.3
Methylobacterium extorquens PA1	79.3	97.3	100.0	78.9	97.3	97.4	97.4	97.4	97.4	97.3	97.4	97.4	93.3	93.3	93.3	97.4
Methylobacterium nodulans ORS 2060	82.5	78.9	78.9	100.0	78.9	79.0	79.0	79.0	79.0	78.9	79.0	79.0	78.9	78.9	78.9	78.9
SLI 223	79.3	99.8	97.3	78.8	100.0	97.4	97.4	97.4	97.4	100.0	97.4	97.4	93.4	93.4	93.4	97.4
SLI 231	79.3	97.4	97.4	78.9	97.4	100.0	100.0	100.0	100.0	97.4	100.0	100.0	93.5	93.5	93.5	97.4
SLI 233	79.3	97.3	97.4	78.9	97.4	100.0	100.0	100.0	100.0	97.4	100.0	100.0	93.5	93.5	93.5	97.4
SLI 274	79.3	97.4	97.4	78.9	97.4	100.0	100.0	100.0	100.0	97.4	100.0	100.0	93.6	93.6	93.6	97.4
SLI 285	79.4	97.4	97.4	78.9	97.4	100.0	100.0	100.0	100.0	97.4	100.0	100.0	93.5	93.5	93.5	97.4
SLI 384	79.3	99.8	97.3	78.8	100.0	97.4	97.4	97.4	97.4	100.0	97.4	97.4	93.4	93.4	93.4	97.4
SLI 499	79.4	97.4	97.4	78.9	97.4	100.0	100.0	100.0	100.0	97.4	100.0	100.0	93.5	93.5	93.5	97.4
SLI 505	79.3	97.4	97.4	78.9	97.4	100.0	100.0	100.0	100.0	97.4	100.0	100.0	93.5	93.5	93.5	97.4
SLI 516	79.2	93.3	93.3	78.9	93.4	93.5	93.5	93.5	93.5	93.4	93.5	93.5	100.0	100.0	100.0	93.4
SLI 575	79.2	93.3	93.3	78.9	93.4	93.5	93.5	93.5	93.5	93.4	93.5	93.5	100.0	100.0	100.0	93.4
SLI 576	79.2	93.3	93.3	78.9	93.4	93.5	93.5	93.5	93.5	93.4	93.5	93.5	100.0	100.0	100.0	93.4
SLI 716	79.3	97.3	97.4	78.9	97.4	97.4	97.4	97.4	97.4	97.4	97.4	97.4	93.4	93.4	93.4	100.0

Figure 1. Phylogenetic and taxonomic characterization of a methylotrophic community isolated from the soybean phyllosphere. (**A**) Phylogenetic tree based on *rpoB* sequences. Untrimmed *rpoB* sequences from each isolate as well as from reference *Methylobacterium* and related species were obtained from IMG, aligned using MUSCLE, and the Maximum-Likelihood trees were constructed with 100 bootstrap replications using MEGA. Groupings indicate clade identity for each strain (**B**) Average nucleotide identity of all SLI strains compared to representative species from the *extorquens*, *nodulans*, and *aquaticum* clades. All pairwise comparison ANIs found in **Table S1**

Table 2. Distribution of substrate-utilization capabilities of SLI community. All 344 isolates were grown in liquid minimal salts media containing either C_1 (20 mM methanol, 15 mM methylamine, 1 mM dimethylsulfide), C_2 (34 mM ethanol, 5 mM potassium oxalate), sugar (25 mM fructose, 25 mM glucose), or complex insoluble substrates (vanillic acid, cellulose, lignin, tyrosine)

	Substrate	No. of SLI strains
C_1 Substrates	Methanol	344
	Methylamine	344
	Dimethylsulfide	0
C_2 Substrates	Ethanol	344
	Potassium Oxalate	0
Sugars	Glucose	0
	Fructose	10
Insoluble C_{2+} Substrates	Vanillic Acid	78
	Lignin	0
	Cellulose	0
	Tyrosine	0

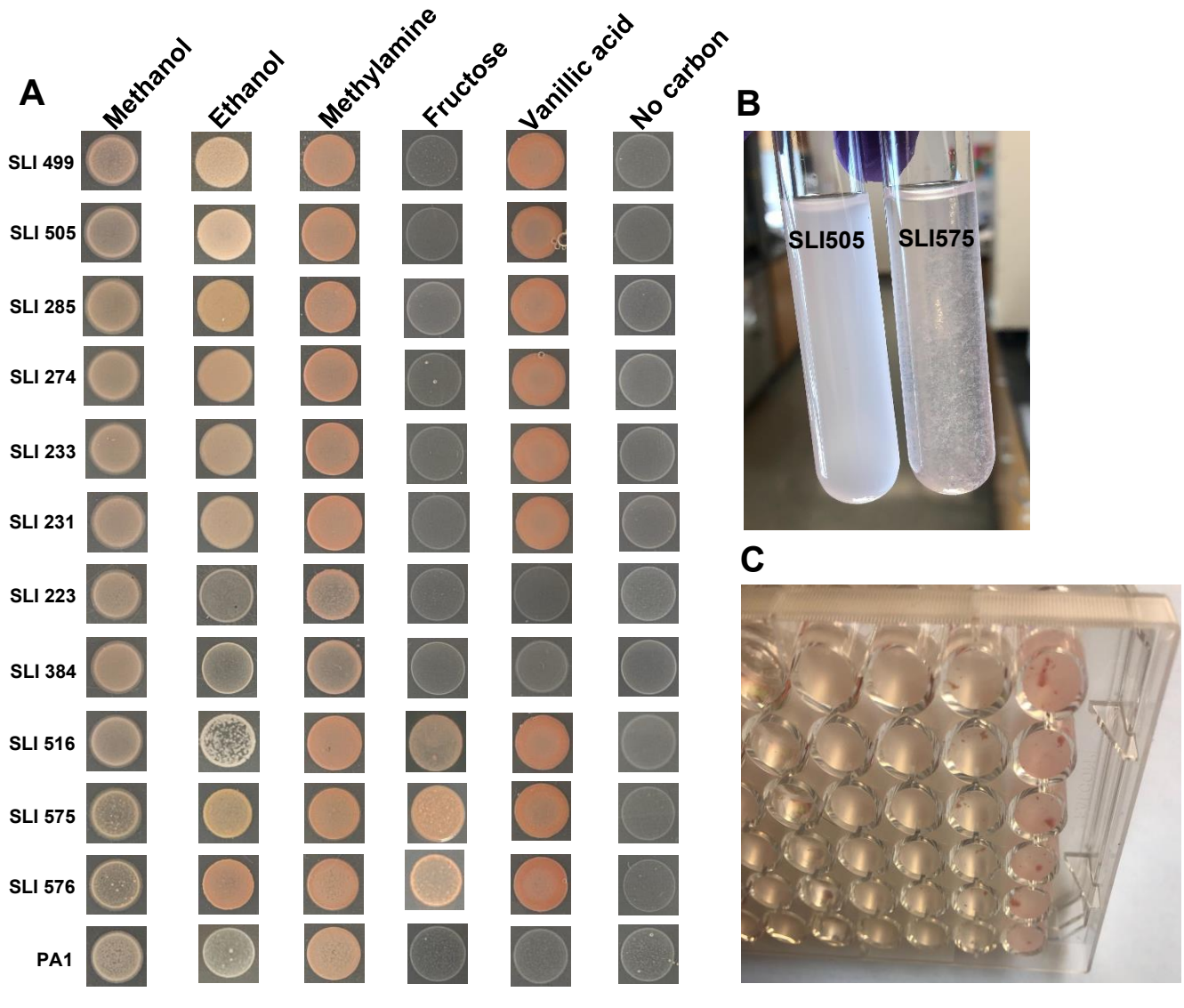

Figure 2. (A) Spotting of a subset of SLI strains on various substrates to demonstrate differential metabolic capabilities of SLI test cohort. All strains were spotted on minimal agar supplemented with either 20 mM methanol, 34 mM methanol, 15 mM methylamine, 5 mM vanillic acid, 25 mM fructose, or no carbon. *Methylobacterium extorquens* PA1Δ*cel* as a comparison of known substrate utilization capabilities in a model *extorquens* clade strain. Biofilm formation of SLI 575 in liquid culture **(B)** and in microplates (**C**)

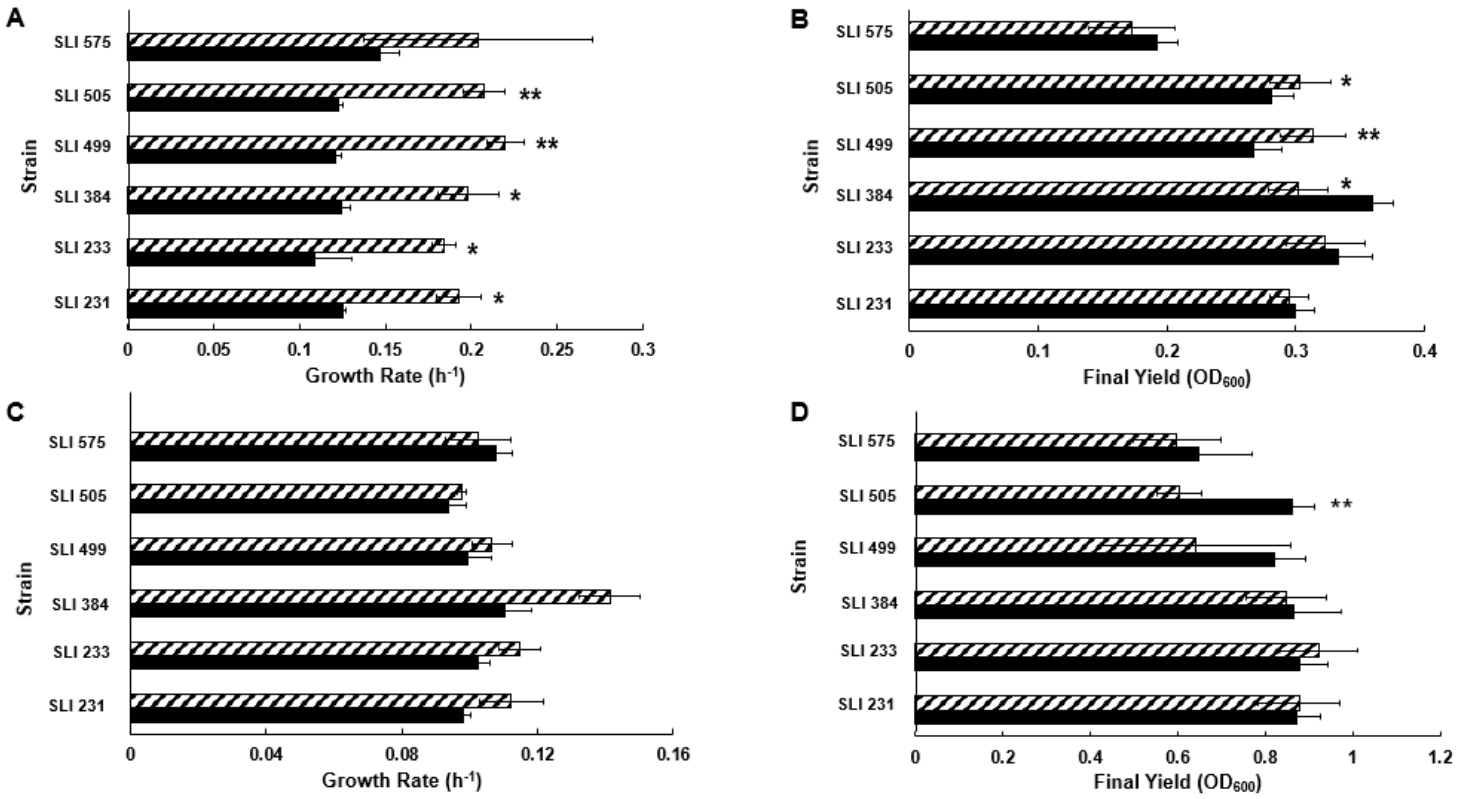

767

768 **Figure 3.** Growth phenotypes of SLI test cohort on alcohols in the presence and absence of La^{3+}.

769 (**A**) Growth rates on 20 mM methanol +/- 2 µM $LaCl_3$ (**B**) Final yields on 20 mM methanol +/- 2

770 µM $LaCl_3$ (**C**) Growth rates on 34 mM ethanol +/-2 µM $LaCl_3$ (**D**) Final yields on 34 mM

771 ethanol +/- 2 µM $LaCl_3$. Black bars (bottom) represent cultures grown in the absence of $LaCl_3$;

772 hatched bars (top) represent cultures grown in the presence of $LaCl_3$. N=3. Error bars represent

773 standard deviation. Significant differences for each strain +/- $LaCl_3$ determined by Student's

774 paired t-test (*, $p<0.05$; **, $p<0.01$). Significant differences between all strains +/- $LaCl_3$

775 determined using one-way ANOVA with post-hoc Tukey HSD (**Table S3**)

776

777

778

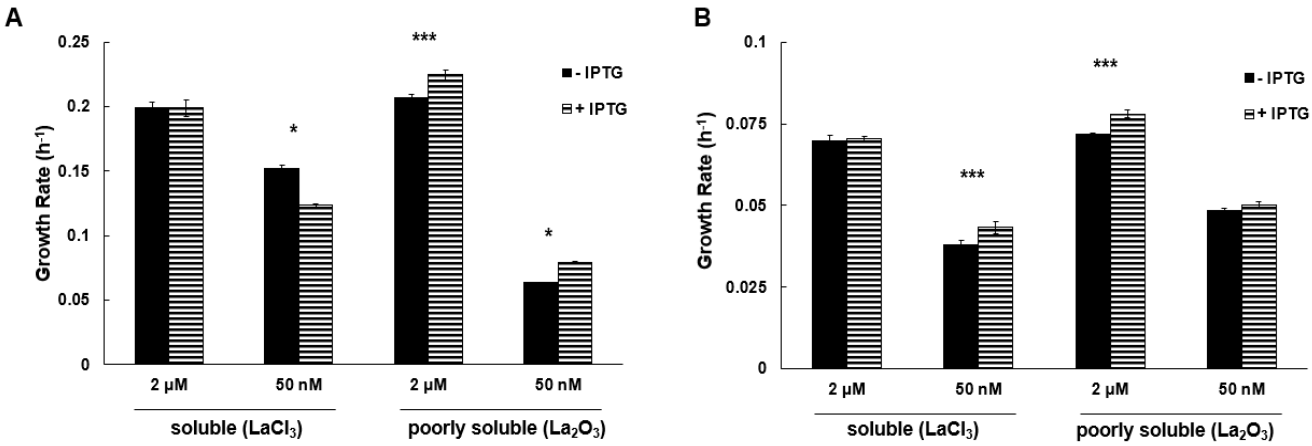

779

780 **Figure 4.** Growth phenotypes of lanmodulin expression in SLI 575 (**A)** Growth rates of IPTG-

781 induced *lanM* expression in SLI 575 on 20 mM methanol with 2 uM or 50 nM $LaCl_3$ or La_2O_3

782 (**B)** Growth rates of IPTG-induced *lanM* expression in SLI 575 on 34 mM ethanol with 2 uM or

783 50 nM $LaCl_3$ or La_2O_3. Striped bars (right) indicate *lanM* expression induced with 1 mM IPTG.

784 N=2-4. Error bars represent standard deviation. Significant differences for each strain +/- 1 mM

785 IPTG determined by Student's paired t-test (*, $p<0.05$; **, $p<0.01$; ***, $p<0.001$)

786

787

788

789

790

791

792

793

794

795

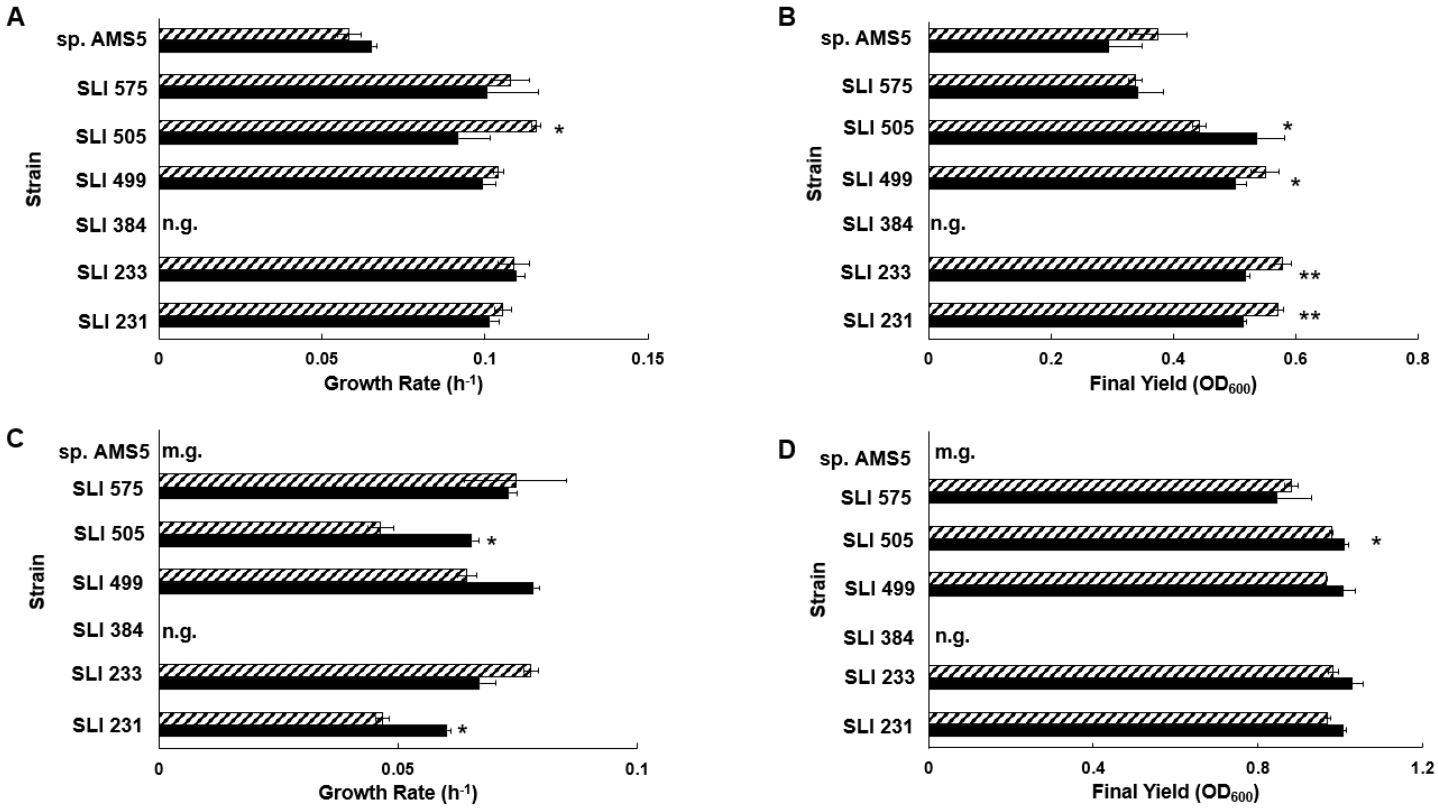

796

797 **Figure 5.** Growth phenotypes of SLI test cohort and *Methylobacterium sp.* AMS5 on vanillic

798 acid in the presence and absence of La^{3+}. (**A**) Growth rates on 5 mM vanillic acid +/- 2 μM $LaCl_3$

799 (**B**) Final yields on 5 mM vanillic acid +/- 2 μM $LaCl_3$ (**C)** Growth rates on 12 mM vanillic acid

800 +/- 2 μM $LaCl_3$ (**D**) Final yields on 12 mM vanillic acid +/- 2 μM $LaCl_3$. n.g., no growth; m.g.,

801 minimal growth (<OD_{600} 0.2). Black bars (bottom) represent cultures grown in the absence of

802 $LaCl_3$; hatched bars (top) represent cultures grown in the presence of $LaCl_3$. N=3. Error bars

803 represent standard deviation. Significant differences for each strain +/- $LaCl_3$ determined by

804 Student's paired t-test (*, $p<0.05$; **, $p<0.01$). Significant differences between all strains +/-

805 $LaCl_3$ determined using one-way ANOVA with post-hoc Tukey HSD (**Table S3**)

806

807

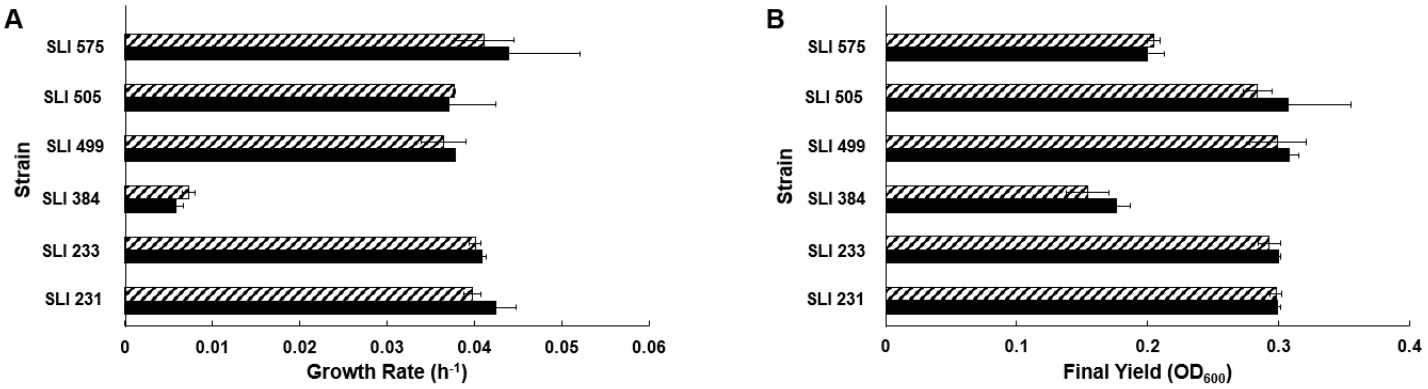

Figure 6. Growth phenotypes of SLI test cohort on methylamine in the presence and absence of La^{3+}. (**A**) Growth rates on 15 mM methylamine +/- 2 μM $LaCl_3$ (**B**) Final yields on 15 mM methylamine +/- 2 μM $LaCl_3$. Black bars (bottom) represent cultures grown in the absence of $LaCl_3$; hatched bars (top) represent cultures grown in the presence of $LaCl_3$. N=3. Error bars represent standard deviation. Significant differences for each strain +/- $LaCl_3$ determined by Student's paired t-test. Significant differences between all strains +/- $LaCl_3$3 determined using one-way ANOVA with post-hoc Tukey HSD (**Table S3**)

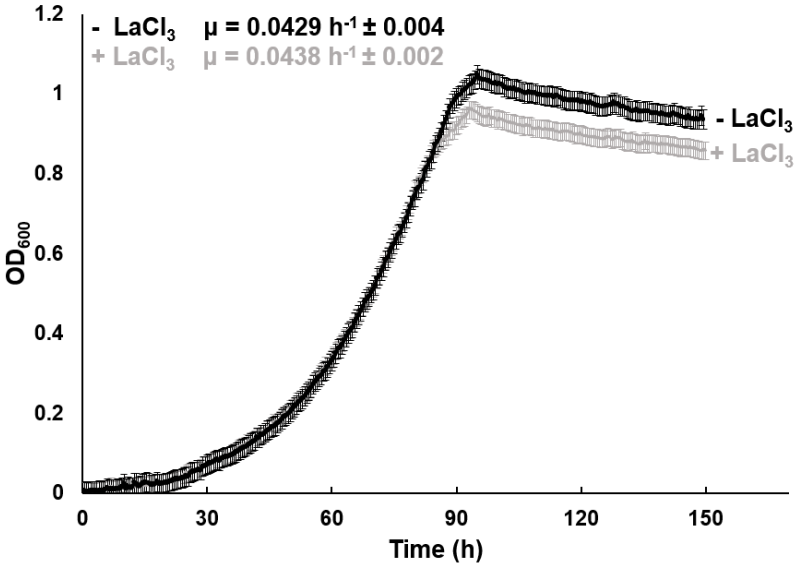

Figure 7. Growth curves of SLI 575 on 25 mM fructose +/- 2 μM $LaCl_3$. N=4. Error bars represent standard deviation

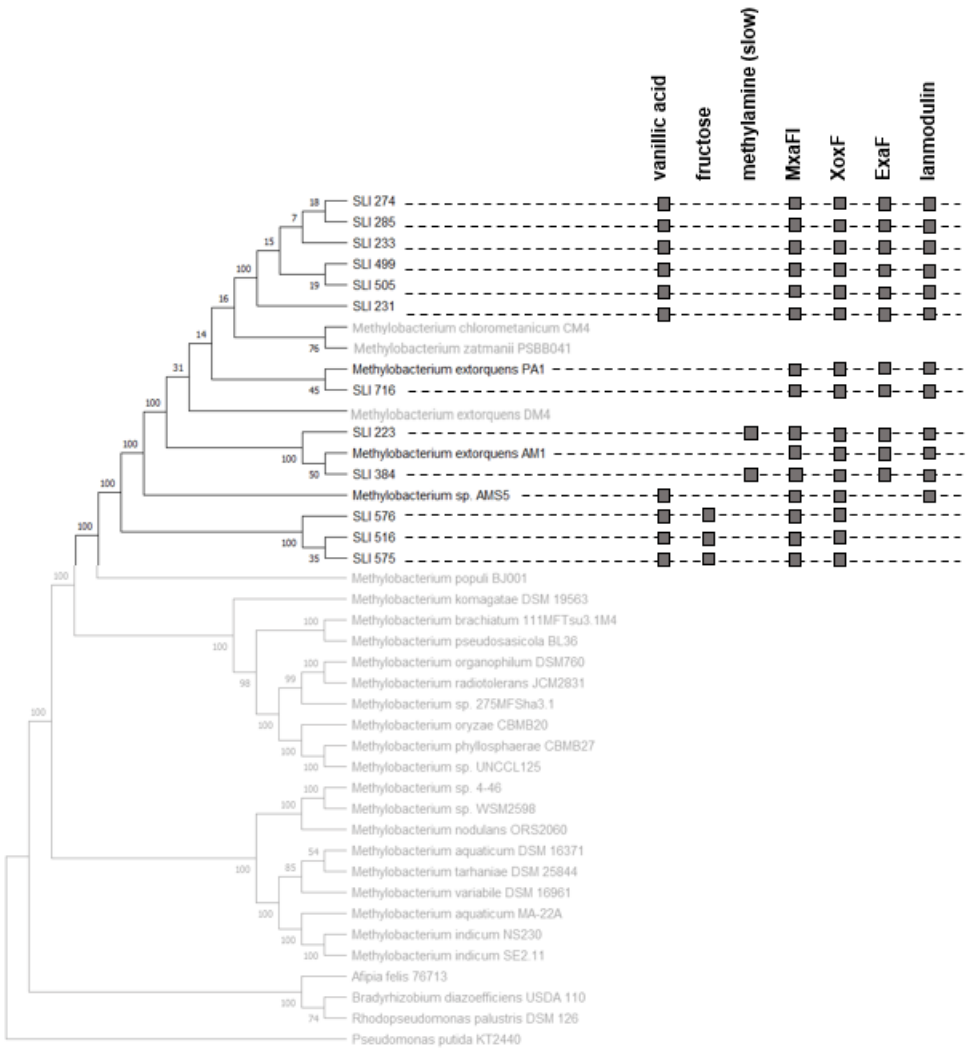

Figure 8. Metabolic capabilities (growth on vanillic acid, growth on fructose, slow growth on methylamine) and lanthanide-related gene products (MxaFI, XoxF, ExaF, lanmodulin) present in SLI strains and model *extorquens* clade species referenced in this study (*M. extorquens* AM1, *M. extorquens* PA1, *M. sp.* AMS5). Phylogenetic tree modified from **Figure 1A**

Table S1. Average nucleotide identity of all 11 SLI strains compared to evolutionarily-related methylotroph and non-methylotrophic species, including all species represented in phylogenetic tree from **Figure 1.** A, *Afipia felis* 76713; B, *Bradyrhizobium diazoefficiens* USDA 110; C, *Methylobacterium aquaticum* DSM 16371; D, *Methylobacterium aquaticum* MA-22A; E, *Methylobacterium brachiatum* 111MFTsu3.1M4; F, *Methylobacterium chloromethanicum* CM4; G, *Methylobacterium extorquens* AM1; H, *Methylobacterium extorquens* DM4; I, *Methylobacterium extorquens* PA1; J, *Methylobacterium indicum* NS230; K, *Methylobacterium indicum* SE2,11; L, *Methylobacterium komagatae* DSM 19563; M, *Methylobacterium nodulans* ORS 2060; N, *Methylobacterium organophilum* DSM 760; O, *Methylobacterium oryzae* CBMB20; P, *Methylobacterium phyllosphaerae* CBMB27; Q, *Methylobacterium platani* JCM 14648; R, *Methylobacterium populi* BJ001; S, *Methylobacterium pseudosasicola* BL36; T, *Methylobacterium radiotolerans* JCM 2831; U, *Methylobacterium* sp. 275MFSha3.1; V, *Methylobacterium* sp. 4-46; W, *Methylobacterium* sp. AMS5; X, *Methylobacterium* sp. UNCCL125; Y, *Methylobacterium* sp. WSM2598; Z, *Methylobacterium* tarhaniae DSM 25844; AA, *Methylobacterium* variabile DSM 16961; AB, *Methylobacterium* zatmanii PSBB041; AC, *Pseudomonas putida* KT2440; AD, *Rhodopseudomonas palustris* DSM 126; AE, SLI 223; AF, SLI 231; AG, SLI 233; AH, SLI 274; AI, SLI 285; AJ, SLI 384; AK, SLI 499; AL, SLI 505; AM, SLI 516; AN, SLI 575; AO, SLI 576

	A	B	C	D	E	F	G	H	I	J	K	L	M	N	O	P	Q	R	S	T	U	V	W	X	Y	Z	AA	AB	AC	AD	AE	AF	AG	AH	AI	AJ	AK	AL	AM	AN	AO
A	100	78	75	75	75	75	75	75	76	76	75	75	75	75	75	75	78	76	75	75	75	75	76	75	75	76	76	75	72	78	76	76	75	75	75	76	76	76	75	75	75
B	78	100	76	76	76	76	76	76	76	76	76	75	76	76	75	75	78	76	76	76	76	76	76	75	76	76	76	76	72	80	76	76	76	76	76	76	76	76	76	76	76
C	75	76	100	89	79	80	79	80	79	89	89	79	82	80	79	79	93	80	79	79	79	82	79	79	82	91	89	79	73	76	79	79	79	79	79	79	79	79	79	79	79
D	75	76	89	100	79	79	79	80	79	79	93	79	82	80	79	79	93	80	79	80	80	83	79	80	83	90	89	79	73	76	79	79	79	79	79	79	79	79	79	79	79
E	75	76	79	79	100	80	80	80	80	79	80	81	79	86	86	86	84	80	92	86	86	79	80	86	79	79	80	80	72	76	80	80	80	80	80	80	80	80	80	80	80
F	75	76	80	79	80	100	97	97	97	79	79	80	79	80	80	80	84	90	80	80	80	79	95	80	79	79	80	97	72	76	97	97	97	97	97	97	97	97	93	93	93
G	75	76	79	79	80	97	100	97	97	79	79	80	79	80	80	80	84	90	80	80	80	79	95	80	79	79	80	97	72	76	100	97	97	97	97	100	97	97	93	93	93
H	75	76	80	79	80	97	97	100	97	79	79	80	79	80	80	80	84	90	80	80	80	79	95	80	79	79	80	97	72	76	97	97	97	97	97	97	97	97	93	93	93
I	76	76	79	79	80	97	97	97	100	79	79	79	79	80	80	80	84	90	80	80	80	79	95	80	79	79	79	97	72	76	97	97	97	97	97	97	97	97	93	93	93
J	76	76	89	93	79	79	79	79	79	100	99	79	83	80	79	79	93	80	79	80	79	83	79	79	83	90	89	79	73	76	79	79	79	79	79	79	79	79	79	79	79
K	75	76	89	79	80	79	79	79	79	99	100	79	83	80	79	79	93	80	79	80	80	83	79	79	83	90	89	79	73	76	79	79	79	79	79	79	79	79	79	79	79

L	75	75	79	79	81	80	80	80	79	79	79	100	78	83	81	81	84	80	81	82	82	78	79	82	78	79	79	79	72	75	79	79	79	79	79	79	79	79	79	79	79
M	75	76	82	82	79	79	79	79	79	83	83	78	100	79	79	79	87	79	79	79	79	86	79	79	86	82	83	79	72	76	79	79	79	79	79	79	79	79	79	79	79
N	75	76	80	80	86	80	80	80	80	80	80	83	79	100	91	91	84	81	86	99	95	80	80	91	80	80	80	80	73	76	80	80	80	80	80	80	80	80	80	80	80
O	75	75	79	79	86	80	80	80	80	79	79	81	79	91	100	99	84	80	86	91	91	79	80	99	79	79	80	80	72	76	80	80	80	80	80	80	80	80	80	80	80
P	75	76	79	79	86	80	80	80	80	79	79	81	79	91	99	100	84	80	86	91	91	79	80	99	79	79	80	80	73	76	80	80	80	80	80	80	80	80	80	80	80
Q	78	78	93	93	84	84	84	84	84	93	93	83	87	84	84	84	100	84	84	85	84	87	84	84	87	93	92	84	75	78	84	84	84	84	84	84	84	84	84	84	84
R	76	76	80	80	80	90	90	90	90	80	80	80	79	81	80	80	84	100	80	81	80	79	90	80	79	80	80	90	72	76	90	90	90	90	90	90	90	90	90	90	90
S	75	76	79	79	92	80	80	80	80	79	79	81	79	86	86	86	84	80	100	86	86	79	80	86	79	79	79	80	73	76	80	80	80	80	80	80	80	80	80	80	80
T	75	76	79	80	86	80	80	80	80	80	80	82	79	99	91	91	85	81	86	100	95	80	80	91	80	80	80	80	73	76	80	80	80	80	80	80	80	80	80	80	80
U	75	76	79	80	86	80	80	80	80	80	80	82	79	95	91	91	84	80	86	95	100	80	80	91	80	80	80	80	73	76	80	80	80	80	80	80	80	80	80	80	80
V	75	76	82	83	79	79	79	79	79	83	83	78	86	80	79	79	87	79	79	80	80	100	79	79	79	83	83	79	72	76	79	79	79	79	79	79	79	79	79	79	79
W	75	76	79	79	80	95	95	95	95	79	79	79	79	80	80	80	84	90	80	80	80	79	100	80	79	79	79	95	72	76	95	95	95	95	95	95	95	95	93	93	93

X	75	76	79	80	86	80	80	80	80	79	79	82	79	91	99	99	84	80	86	91	91	79	80	100	79	79	80	80	73	76	80	80	80	80	80	80	80	80	80	80	80
Y	75	76	82	83	79	79	79	79	79	83	83	78	86	80	79	79	87	79	79	80	80	99	79	79	100	83	83	79	72	76	79	79	79	79	79	79	79	79	79	79	79
Z	76	76	91	90	79	79	79	79	79	90	90	79	82	80	79	79	93	80	79	80	80	83	79	79	83	100	90	79	73	76	79	79	79	79	79	79	79	79	79	79	79
AA	76	76	89	89	80	80	80	80	79	89	89	79	83	80	80	80	92	80	79	80	80	83	79	80	83	90	100	80	73	76	79	79	79	79	79	79	79	79	79	79	79
AB	75	76	79	79	80	97	97	97	97	79	79	79	79	80	80	80	84	90	80	80	80	79	95	80	79	79	80	100	72	76	97	97	97	97	97	97	97	97	93	93	93
AC	72	72	73	73	72	72	72	72	72	73	73	72	72	73	72	73	75	72	73	73	73	72	72	73	72	73	73	72	100	72	72	72	72	72	72	72	72	72	72	72	72
AD	78	80	76	76	76	76	76	76	76	76	76	75	76	76	76	76	78	76	76	76	76	76	76	76	76	76	76	76	72	100	76	76	76	76	76	76	76	76	76	76	76
AE	76	76	79	79	80	97	100	97	97	79	79	79	79	80	80	80	84	90	80	80	80	79	95	80	79	79	79	97	72	76	100	97	97	97	97	100	97	97	93	93	93
AF	76	76	79	79	80	97	97	97	97	79	79	79	79	80	80	80	84	90	80	80	80	79	95	80	79	79	79	97	72	76	97	100	100	100	100	97	100	100	94	94	94
AG	76	76	79	79	80	97	97	97	97	79	79	79	79	80	80	80	84	90	80	80	80	79	95	80	79	79	79	97	72	76	97	100	100	100	100	97	100	100	94	94	94
AH	76	76	79	79	80	97	97	97	97	79	79	79	79	80	80	80	84	90	80	80	80	79	95	80	79	79	79	97	72	76	97	100	100	100	100	97	100	100	94	94	94
AI	76	76	79	79	80	97	97	97	97	79	79	79	79	80	80	80	84	90	80	80	80	79	95	80	79	79	79	97	72	76	97	100	100	100	100	97	100	100	94	94	94

AJ	76	76	79	79	80	97	100	97	97	79	79	79	79	80	80	80	84	90	80	80	80	79	95	80	79	79	79	97	72	76	100	97	97	97	97	100	97	97	93	93	93
AK	76	76	79	79	80	97	97	97	97	79	79	79	79	80	80	80	84	90	80	80	80	79	95	80	79	79	79	97	72	76	97	100	100	100	100	97	100	100	94	94	94
AL	76	76	79	79	80	97	97	97	97	79	79	79	79	80	80	80	84	90	80	80	80	79	95	80	79	79	79	97	72	76	97	100	100	100	100	97	100	100	94	94	94
AM	75	76	79	79	80	93	93	93	93	79	79	79	79	80	80	80	84	90	80	80	80	79	93	80	79	79	79	93	72	76	93	94	94	94	94	93	94	94	100	100	100
AN	75	76	79	79	80	93	93	93	93	79	79	79	79	80	80	80	84	90	80	80	80	79	93	80	79	79	79	93	72	76	93	94	94	94	94	93	94	94	100	100	100
AO	75	76	79	79	80	93	93	93	93	79	79	79	79	80	80	80	84	90	80	80	80	79	93	80	79	79	79	93	72	76	93	94	94	94	94	93	94	94	100	100	100

877

878 **Table S2**. Summary of metabolic and lanthanide-related genes present in SLI strains, using *M. extorquens* AM1 and PA1 as reference

879 strains

880

		Strain												
		M. extorquens AM1	*M. extorquens* PA1	SLI 223	SLI 231	SLI 233	SLI 274	SLI 285	SLI 384	SLI 499	SLI 505	SLI 516	SLI 575	SLI 576
PQQ-dep. alcohol dehydrogenases	*mxaF*	✓	✓	✓	✓	✓	✓	✓	✓	✓	✓	✓	✓	✓
	mxaI	✓	✓	✓	✓	✓	✓	✓	✓	✓	✓	✓	✓	✓
	mxaG	✓	✓	✓	✓	✓	✓	✓	✓	✓	✓	✓	✓	✓
	xoxF1	✓	✓	✓	✓	✓	✓	✓	✓	✓	✓	✓	✓	✓
	xoxG	✓	✓	✓	✓	✓	✓	✓	✓	✓	✓	✓	✓	✓
	xoxF2	✓	✓	✓	✓	✓	✓	✓	✓	✓	✓	✓	✓	✓
	exaF	✓	✓	✓	✓	✓	✓	✓	✓	✓	✓	-	-	-
	exaG	✓	✓	✓	✓	✓	✓	✓	✓	✓	✓	-	-	-
Formaldehyde oxidation pathway	*fae1*	✓	✓	✓	✓	✓	✓	✓	✓	✓	✓	✓	✓	✓
	fae2	✓	✓	✓	✓	✓	✓	✓	✓	✓	✓	✓	✓	✓
	fae3	✓	✓	✓	✓	✓	✓	✓	✓	✓	✓	✓	✓	✓
	mtdA	✓	✓	✓	✓	✓	✓	✓	✓	✓	✓	✓	✓	✓
	mtdB	✓	✓	✓	✓	✓	✓	✓	✓	✓	✓	✓	✓	✓
	mch	✓	✓	✓	✓	✓	✓	✓	✓	✓	✓	✓	✓	✓
	fhcA	✓	✓	✓	✓	✓	✓	✓	✓	✓	✓	✓	✓	✓
	fhcB	✓	✓	✓	✓	✓	✓	✓	✓	✓	✓	✓	✓	✓
	fhcC	✓	✓	✓	✓	✓	✓	✓	✓	✓	✓	✓	✓	✓
	fhcD	✓	✓	✓	✓	✓	✓	✓	✓	✓	✓	✓	✓	✓
Formate dehydrogenases	*fdh1A*	✓	✓	✓	✓	✓	✓	✓	✓	✓	✓	-	-	-
	fdh1B	✓	✓	✓	✓	✓	✓	✓	✓	✓	✓	-	-	-
	fdh2A	✓	✓	✓	✓	✓	✓	✓	✓	✓	✓	✓	✓	✓
	fdh2B	✓	✓	✓	✓	✓	✓	✓	✓	✓	✓	✓	✓	✓
	fdh2C	✓	✓	✓	✓	✓	✓	✓	✓	✓	✓	✓	✓	✓
	fdh2D	✓	✓	✓	✓	✓	✓	✓	✓	✓	✓	✓	✓	✓
	fdh3A	✓	✓	✓	✓	✓	✓	✓	✓	✓	✓	✓	✓	✓
	fdh3B	✓	✓	✓	✓	✓	✓	✓	✓	✓	✓	✓	✓	✓
	fdh4A	✓	✓	✓	✓	✓	✓	✓	✓	✓	✓	✓	✓	✓
	fdh4B	✓	✓	✓	✓	✓	✓	✓	✓	✓	✓	✓	✓	✓
Formate assimilation & serine cycle	*mtdA*	✓	✓	✓	✓	✓	✓	✓	✓	✓	✓	✓	✓	✓
	fch	✓	✓	✓	✓	✓	✓	✓	✓	✓	✓	✓	✓	✓
	ftfL	✓	✓	✓	✓	✓	✓	✓	✓	✓	✓	✓	✓	✓
	sga	✓	✓	✓	✓	✓	✓	✓	✓	✓	✓	✓	✓	✓
	glyA	✓	✓	✓	✓	✓	✓	✓	✓	✓	✓	✓	✓	✓
	hpr	✓	✓	✓	✓	✓	✓	✓	✓	✓	✓	✓	✓	✓
RuMP cycle	*hps*	-	-	-	-	-	-	-	-	-	-	-	-	-
	phi	-	-	-	-	-	-	-	-	-	-	-	-	-
	pfk	-	-	-	-	-	-	-	-	-	-	✓	✓	✓
	fba	✓	✓	✓	✓	✓	✓	✓	✓	✓	✓	✓	✓	✓

881

882

883

		Strain												
		M. extorquens AM1	*M. extorquens* PA1	SLI 223	SLI 231	SLI 233	SLI 274	SLI 285	SLI 384	SLI 499	SLI 505	SLI 516	SLI 575	SLI 576
Methylamine dehydrogenase	*mauF*	✓	-	-	-	-	-	-	-	-	-	-	-	-
	mauB	✓	-	-	-	-	-	-	-	-	-	-	-	-
	mauE	✓	-	-	-	-	-	-	-	-	-	-	-	-
	mauD	✓	-	-	-	-	-	-	-	-	-	-	-	-
	mauA	✓	-	-	-	-	-	-	-	-	-	-	-	-
	mauC	✓	-	-	-	-	-	-	-	-	-	-	-	-
	mauJ	✓	-	-	-	-	-	-	-	-	-	-	-	-
	mauG	✓	-	-	-	-	-	-	-	-	-	-	-	-
	mauL	✓	-	-	-	-	-	-	-	-	-	-	-	-
	mauM	✓	-	-	-	-	-	-	-	-	-	-	-	-
	mauN	✓	-	-	-	-	-	-	-	-	-	-	-	-
N-methylglutamate pathway	*mgdD*	✓	✓	✓	✓	✓	✓	✓	✓	✓	✓	✓	✓	✓
	mgdC	✓	✓	✓	✓	✓	✓	✓	✓	✓	✓	✓	✓	✓
	mgdB	✓	✓	✓	✓	✓	✓	✓	✓	✓	✓	✓	✓	✓
	mgdA	✓	✓	✓	✓	✓	✓	✓	✓	✓	✓	✓	✓	✓
	mgsA	✓	✓	✓	✓	✓	✓	✓	✓	✓	✓	✓	✓	✓
	mgsB	✓	✓	✓	✓	✓	✓	✓	✓	✓	✓	✓	✓	✓
	mgsC	✓	✓	✓	✓	✓	✓	✓	✓	✓	✓	✓	✓	✓
	gmaS	✓	✓	✓	✓	✓	✓	✓	✓	✓	✓	✓	✓	✓
Aromatic acid catabolism gene island	*ech*	-	-	-	✓	✓	✓	✓	-	✓	✓	✓	✓	✓
	vdh	-	-	-	✓	✓	✓	✓	-	✓	✓	✓	✓	✓
	vanA	-	-	-	✓	✓	✓	✓	-	✓	✓	✓	✓	✓
	vanB	-	-	-	✓	✓	✓	✓	-	✓	✓	✓	✓	✓
	pobA	-	-	-	✓	✓	✓	✓	-	✓	✓	✓	✓	✓
	pcaG	-	-	-	✓	✓	✓	✓	-	✓	✓	✓	✓	✓
	pcaH	-	-	-	✓	✓	✓	✓	-	✓	✓	✓	✓	✓
	vanR	-	-	-	✓	✓	✓	✓	-	✓	✓	✓	✓	✓
	pcaK	-	-	-	✓	✓	✓	✓	-	✓	✓	✓	✓	✓
	pcaB	-	-	-	✓	✓	✓	✓	-	✓	✓	✓	✓	✓
	pcaC	-	-	-	✓	✓	✓	✓	-	✓	✓	✓	✓	✓
	pcaD	-	-	-	✓	✓	✓	✓	-	✓	✓	✓	✓	✓
	pcaIJ	-	-	-	✓	✓	✓	✓	-	✓	✓	✓	✓	✓
	pcaF	-	-	-	✓	✓	✓	✓	-	✓	✓	✓	✓	✓

884

		Strain												
		M. extorquens AM1	*M. extorquens* PA1	SLI 223	SLI 231	SLI 233	SLI 274	SLI 285	SLI 384	SLI 499	SLI 505	SLI 516	SLI 575	SLI 576
Methylolanthanin Cluster	*mluA*	✓	✓	✓	✓	✓	✓	✓	✓	✓	✓	✓	✓	✓
	mluR	✓	✓	✓	✓	✓	✓	✓	✓	✓	✓	✓	✓	✓
	mluI	✓	✓	✓	✓	✓	✓	✓	✓	✓	✓	✓	✓	✓
	mllA	✓	✓	✓	✓	✓	✓	✓	✓	✓	✓	✓	✓	✓
	mllBC	✓	✓	✓	✓	✓	✓	✓	✓	✓	✓	✓	✓	✓
	mllDE	✓	✓	✓	✓	✓	✓	✓	✓	✓	✓	✓	✓	✓
	mllF	✓	✓	✓	✓	✓	✓	✓	✓	✓	✓	✓	✓	✓
	mllG	✓	✓	✓	✓	✓	✓	✓	✓	✓	✓	✓	✓	✓
	mllH	✓	✓	✓	✓	✓	✓	✓	✓	✓	✓	✓	✓	✓
	mllJ	✓	✓	✓	✓	✓	✓	✓	✓	✓	✓	✓	✓	✓
Lanthanide Utilization and Transport	*lutA*	✓	✓	✓	✓	✓	✓	✓	✓	✓	✓	✓	✓	✓
	lutB	✓	✓	✓	✓	✓	✓	✓	✓	✓	✓	✓	✓	✓
	lutC	✓	✓	✓	✓	✓	✓	✓	✓	✓	✓	✓	✓	✓
	lutD	✓	✓	✓	✓	✓	✓	✓	✓	✓	✓	✓	✓	✓
	lutE	✓	✓	✓	✓	✓	✓	✓	✓	✓	✓	✓	✓	✓
	lutF	✓	✓	✓	✓	✓	✓	✓	✓	✓	✓	✓	✓	✓
	lutG	✓	✓	✓	✓	✓	✓	✓	✓	✓	✓	✓	✓	✓
	lutH	✓	✓	✓	✓	✓	✓	✓	✓	✓	✓	✓	✓	✓
	lanM	✓	✓	✓	✓	✓	✓	✓	✓	✓	✓	-	-	-
	lutI	✓	✓	✓	✓	✓	✓	✓	✓	✓	✓	✓	✓	✓
Ln Switch	*mxcQ*	✓	✓	✓	✓	✓	✓	✓	✓	✓	✓	✓	✓	✓
	mxcE	✓	✓	✓	✓	✓	✓	✓	✓	✓	✓	✓	✓	✓
	mxbD	✓	✓	✓	✓	✓	✓	✓	✓	✓	✓	✓	✓	✓
	mxbM	✓	✓	✓	✓	✓	✓	✓	✓	✓	✓	✓	✓	✓

885

886 **Table S3.** Significant differences in growth rates and final yields between all strains on 20 mM
887 methanol **(Figure 3) ,** 34 mM ethanol **(Figure 3),** 5 and 12 mM vanillic acid (**Figure 5**), 15 mM
888 methylamine **(Figure 6**) +/- $LaCl_3$ determined using one-way ANOVA with post-hoc Tukey
889 HSD. Significant differences for each strain +/- $LaCl_3$ or +/- IPTG for lanmodulin expression
890 phenotypes (**Figure 4**) determined by Student's paired t-test

20 mM Methanol ± $LaCl_3$			
Growth Rate		**Final Yield**	
Comparison	**p-value**	**Comparison**	**p-value**
SLI 231 ± $LaCl_3$	0.005752	SLI 231 ± $LaCl_3$	0.1264
SLI 233 ± $LaCl_3$	0.002731	SLI 233 ± $LaCl_3$	0.4189
SLI 384 ± $LaCl_3$	0.6598	SLI 384 ± $LaCl_3$	0.6513
SLI 499 ± $LaCl_3$	0.00311	SLI 499 ± $LaCl_3$	0.2585
SLI 505 ± $LaCl_3$	0.004484	SLI 505 ± $LaCl_3$	0.2158
SLI 575 ± $LaCl_3$	0.00002213	SLI 575 ± $LaCl_3$	0.2463
SLI 231 x SLI 233 - $LaCl_3$	1	SLI 231 x SLI 233 - $LaCl_3$	0.9232
SLI 231 x SLI 384 - $LaCl_3$	0.133	SLI 231 x SLI 384 - $LaCl_3$	0.9546
SLI 231 x SLI 499 - $LaCl_3$	1	SLI 231 x SLI 499 - $LaCl_3$	0.9966
SLI 231 x SLI 505 - $LaCl_3$	0.9998	SLI 231 x SLI 505 - $LaCl_3$	0.6545
SLI 231 x SLI 575 - $LaCl_3$	0.7947	SLI 231 x SLI 575 - $LaCl_3$	0.05092
SLI 233 x SLI 384 - $LaCl_3$	0.1335	SLI 233 x SLI 384 - $LaCl_3$	1
SLI 233 x SLI 499 - $LaCl_3$	1	SLI 233 x SLI 499 - $LaCl_3$	0.9949
SLI 233 x SLI 505 - $LaCl_3$	0.9998	SLI 233 x SLI 505 - $LaCl_3$	0.9861
SLI 233 x SLI 575 - $LaCl_3$	0.7929	SLI 233 x SLI 575 - $LaCl_3$	0.01978
SLI 384 x SLI 499 - $LaCl_3$	0.1097	SLI 384 x SLI 499 - $LaCl_3$	0.9987
SLI 384 x SLI 505 - $LaCl_3$	0.1007	SLI 384 x SLI 505 - $LaCl_3$	0.9702
SLI 384 x SLI 575 - $LaCl_3$	0.03403	SLI 384 x SLI 575 - $LaCl_3$	0.02226
SLI 499 x SLI 505 - $LaCl_3$	1	SLI 499 x SLI 505 - $LaCl_3$	0.8666
SLI 499 x SLI 575 - $LaCl_3$	0.8691	SLI 499 x SLI 575 - $LaCl_3$	0.03202
SLI 505 x SLI 575 - $LaCl_3$	0.8975	SLI 505 x SLI 575 - $LaCl_3$	0.01123
SLI 231 x SLI 233 + $LaCl_3$	0.5873	SLI 231 x SLI 233 + $LaCl_3$	0.9674
SLI 231 x SLI 384 + $LaCl_3$	0.8102	SLI 231 x SLI 384 + $LaCl_3$	0.9996
SLI 231 x SLI 499 + $LaCl_3$	0.9683	SLI 231 x SLI 499 + $LaCl_3$	0.9961
SLI 231 x SLI 505 + $LaCl_3$	0.6435	SLI 231 x SLI 505 + $LaCl_3$	0.07812
SLI 231 x SLI 575 + $LaCl_3$	0.9997	SLI 231 x SLI 575 + $LaCl_3$	0.00001957
SLI 233 x SLI 384 + $LaCl_3$	0.9966	SLI 233 x SLI 384 + $LaCl_3$	0.8901
SLI 233 x SLI 499 + $LaCl_3$	0.28	SLI 233 x SLI 499 + $LaCl_3$	0.82
SLI 233 x SLI 505 + $LaCl_3$	1	SLI 233 x SLI 505 + $LaCl_3$	0.1797
SLI 233 x SLI 575 + $LaCl_3$	0.7234	SLI 233 x SLI 575 + $LaCl_3$	0.00001466
SLI 384 x SLI 499 + $LaCl_3$	0.4465	SLI 384 x SLI 499 + $LaCl_3$	1

SLI 384 x SLI 505 + $LaCl_3$	0.9991	SLI 384 x SLI 505 + $LaCl_3$	0.05721
SLI 384 x SLI 575 + $LaCl_3$	0.9146	SLI 384 x SLI 575 + $LaCl_3$	0.00002191
SLI 499 x SLI 505 + $LaCl_3$	0.3154	SLI 499 x SLI 505 + $LaCl_3$	0.04763
SLI 499 x SLI 575 + $LaCl_3$	0.8993	SLI 499 x SLI 575 + $LaCl_3$	0.00002345
SLI 505 x SLI 575 + $LaCl_3$	0.7776	SLI 505 x SLI 575 + $LaCl_3$	0.00000566

34 mM Ethanol ± $LaCl_3$

Growth Rate		**Final Yield**	
Comparison	**p-value**	**Comparison**	**p-value**
SLI 231 ± $LaCl_3$	0.09398	SLI 231 ± $LaCl_3$	0.9407
SLI 233 ± $LaCl_3$	0.07046	SLI 233 ± $LaCl_3$	0.6408
SLI 384 ± $LaCl_3$	0.08337	SLI 384 ± $LaCl_3$	0.8935
SLI 499 ± $LaCl_3$	0.3597	SLI 499 ± $LaCl_3$	0.2088
SLI 505 ± $LaCl_3$	0.3525	SLI 505 ± $LaCl_3$	0.008165
SLI 575 ± $LaCl_3$	0.5879	SLI 575 ± $LaCl_3$	0.694
SLI 231 x SLI 233 - $LaCl_3$	0.8923	SLI 231 x SLI 233 - $LaCl_3$	1
SLI 231 x SLI 384 - $LaCl_3$	0.1229	SLI 231 x SLI 384 - $LaCl_3$	1
SLI 231 x SLI 499 - $LaCl_3$	0.9989	SLI 231 x SLI 499 - $LaCl_3$	0.9171
SLI 231 x SLI 505 - $LaCl_3$	0.9319	SLI 231 x SLI 505 - $LaCl_3$	1
SLI 231 x SLI 575 - $LaCl_3$	0.2853	SLI 231 x SLI 575 - $LaCl_3$	0.06206
SLI 233 x SLI 384 - $LaCl_3$	0.5211	SLI 233 x SLI 384 - $LaCl_3$	0.9999
SLI 233 x SLI 499 - $LaCl_3$	0.9805	SLI 233 x SLI 499 - $LaCl_3$	0.9522
SLI 233 x SLI 505 - $LaCl_3$	0.4079	SLI 233 x SLI 505 - $LaCl_3$	0.9998
SLI 233 x SLI 575 - $LaCl_3$	0.8289	SLI 233 x SLI 575 - $LaCl_3$	0.05244
SLI 384 x SLI 499 - $LaCl_3$	0.2151	SLI 384 x SLI 499 - $LaCl_3$	0.9858
SLI 384 x SLI 505 - $LaCl_3$	0.02644	SLI 384 x SLI 505 - $LaCl_3$	1
SLI 384 x SLI 575 - $LaCl_3$	0.9918	SLI 384 x SLI 575 - $LaCl_3$	0.07454
SLI 499 x SLI 505 - $LaCl_3$	0.7844	SLI 499 x SLI 505 - $LaCl_3$	0.9889
SLI 499 x SLI 575 - $LaCl_3$	0.4549	SLI 499 x SLI 575 - $LaCl_3$	0.2034
SLI 505 x SLI 575 - $LaCl_3$	0.06793	SLI 505 x SLI 575 - $LaCl_3$	0.07879
SLI 231 x SLI 233 + $LaCl_3$	0.9987	SLI 231 x SLI 233 + $LaCl_3$	0.9963
SLI 231 x SLI 384 + $LaCl_3$	0.004637	SLI 231 x SLI 384 + $LaCl_3$	0.9995
SLI 231 x SLI 499 + $LaCl_3$	0.93	SLI 231 x SLI 499 + $LaCl_3$	0.2218
SLI 231 x SLI 505 + $LaCl_3$	0.2374	SLI 231 x SLI 505 + $LaCl_3$	0.1215
SLI 231 x SLI 575 + $LaCl_3$	0.6082	SLI 231 x SLI 575 + $LaCl_3$	0.111
SLI 233 x SLI 384 + $LaCl_3$	0.008673	SLI 233 x SLI 384 + $LaCl_3$	0.9655
SLI 233 x SLI 499 + $LaCl_3$	0.7734	SLI 233 x SLI 499 + $LaCl_3$	0.1068
SLI 233 x SLI 505 + $LaCl_3$	0.1337	SLI 233 x SLI 505 + $LaCl_3$	0.05601
SLI 233 x SLI 575 + $LaCl_3$	0.4013	SLI 233 x SLI 575 + $LaCl_3$	0.05096
SLI 384 x SLI 499 + $LaCl_3$	0.001055	SLI 384 x SLI 499 + $LaCl_3$	0.3409
SLI 384 x SLI 505 + $LaCl_3$	0.000131	SLI 384 x SLI 505 + $LaCl_3$	0.1958
SLI 384 x SLI 575 + $LaCl_3$	0.000385	SLI 384 x SLI 575 + $LaCl_3$	0.1798
SLI 499 x SLI 505 + $LaCl_3$	0.7021	SLI 499 x SLI 505 + $LaCl_3$	0.9985
SLI 499 x SLI 575 + $LaCl_3$	0.9815	SLI 499 x SLI 575 + $LaCl_3$	0.9971
SLI 505 x SLI 575 + $LaCl_3$	0.9678	SLI 505 x SLI 575 + $LaCl_3$	1

15 mM Methylamine ± $LaCl_3$			
Growth Rate		**Final Yield**	
Comparison	**p-value**	**Comparison**	**p-value**
SLI 231 ± $LaCl_3$	0.2622	SLI 231 ± $LaCl_3$	0.8076
SLI 233 ± $LaCl_3$	0.3036	SLI 233 ± $LaCl_3$	0.3688
SLI 384 ± $LaCl_3$	0.1904	SLI 384 ± $LaCl_3$	0.2502
SLI 499 ± $LaCl_3$	0.5452	SLI 499 ± $LaCl_3$	0.6538
SLI 505 ± $LaCl_3$	0.8891	SLI 505 ± $LaCl_3$	0.5779
SLI 575 ± $LaCl_3$	0.6923	SLI 575 ± $LaCl_3$	0.687
SLI 231 x SLI 233 - $LaCl_3$	0.9982	SLI 231 x SLI 233 - $LaCl_3$	1
SLI 231 x SLI 384 - $LaCl_3$	0.000869	SLI 231 x SLI 384 - $LaCl_3$	0.00843
SLI 231 x SLI 499 - $LaCl_3$	0.8468	SLI 231 x SLI 499 - $LaCl_3$	0.9972
SLI 231 x SLI 505 - $LaCl_3$	0.7692	SLI 231 x SLI 505 - $LaCl_3$	0.9984
SLI 231 x SLI 575 - $LaCl_3$	0.9989	SLI 231 x SLI 575 - $LaCl_3$	0.02364
SLI 233 x SLI 384 - $LaCl_3$	0.001113	SLI 233 x SLI 384 - $LaCl_3$	0.008092
SLI 233 x SLI 499 - $LaCl_3$	0.9659	SLI 233 x SLI 499 - $LaCl_3$	0.9984
SLI 233 x SLI 505 - $LaCl_3$	0.9256	SLI 233 x SLI 505 - $LaCl_3$	0.9991
SLI 233 x SLI 575 - $LaCl_3$	0.9681	SLI 233 x SLI 575 - $LaCl_3$	0.02556
SLI 384 x SLI 499 - $LaCl_3$	0.001847	SLI 384 x SLI 499 - $LaCl_3$	0.005875
SLI 384 x SLI 505 - $LaCl_3$	0.002082	SLI 384 x SLI 505 - $LaCl_3$	0.00611
SLI 384 x SLI 575 - $LaCl_3$	0.0007	SLI 384 x SLI 575 - $LaCl_3$	0.858
SLI 499 x SLI 505 - $LaCl_3$	1	SLI 499 x SLI 505 - $LaCl_3$	1
SLI 499 x SLI 575 - $LaCl_3$	0.6775	SLI 499 x SLI 575 - $LaCl_3$	0.01568
SLI 505 x SLI 575 - $LaCl_3$	0.5903	SLI 505 x SLI 575 - $LaCl_3$	0.0164
SLI 231 x SLI 233 + $LaCl_3$	1	SLI 231 x SLI 233 + $LaCl_3$	0.9982
SLI 231 x SLI 384 + $LaCl_3$	0.00001482	SLI 231 x SLI 384 + $LaCl_3$	0.0002457
SLI 231 x SLI 499 + $LaCl_3$	0.5225	SLI 231 x SLI 499 + $LaCl_3$	1
SLI 231 x SLI 505 + $LaCl_3$	0.845	SLI 231 x SLI 505 + $LaCl_3$	0.869
SLI 231 x SLI 575 + $LaCl_3$	0.9733	SLI 231 x SLI 575 + $LaCl_3$	0.002645
SLI 233 x SLI 384 + $LaCl_3$	0.00001392	SLI 233 x SLI 384 + $LaCl_3$	0.0003005
SLI 233 x SLI 499 + $LaCl_3$	0.4466	SLI 233 x SLI 499 + $LaCl_3$	0.9939
SLI 233 x SLI 505 + $LaCl_3$	0.7702	SLI 233 x SLI 505 + $LaCl_3$	0.9749
SLI 233 x SLI 575 + $LaCl_3$	0.9913	SLI 233 x SLI 575 + $LaCl_3$	0.003543
SLI 384 x SLI 499 + $LaCl_3$	0.0000301	SLI 384 x SLI 499 + $LaCl_3$	0.0002317
SLI 384 x SLI 505 + $LaCl_3$	0.00002318	SLI 384 x SLI 505 + $LaCl_3$	0.0004394
SLI 384 x SLI 575 + $LaCl_3$	0.00001136	SLI 384 x SLI 575 + $LaCl_3$	0.0548
SLI 499 x SLI 505 + $LaCl_3$	0.9809	SLI 499 x SLI 505 + $LaCl_3$	0.8198
SLI 499 x SLI 575 + $LaCl_3$	0.2506	SLI 499 x SLI 575 + $LaCl_3$	0.002429
SLI 505 x SLI 575 + $LaCl_3$	0.4965	SLI 505 x SLI 575 + $LaCl_3$	0.006196
12 mM Vanillic Acid ± $LaCl_3$			
Growth Rate		**Final Yield**	
Comparison	**p-value**	**Comparison**	**p-value**
SLI 231 ± $LaCl_3$	0.02098	SLI 231 ± $LaCl_3$	0.1654

SLI 233 ± $LaCl_3$	0.06785	SLI 233 ± $LaCl_3$	0.35
SLI 499 ± $LaCl_3$	0.1018	SLI 499 ± $LaCl_3$	0.2796
SLI 505 ± $LaCl_3$	0.01559	SLI 505 ± $LaCl_3$	0.01442
SLI 575 ± $LaCl_3$	0.8571	SLI 575 ± $LaCl_3$	0.6117
SLI 231 x SLI 233 - $LaCl_3$	0.05422	SLI 231 x SLI 233 - $LaCl_3$	0.9758
SLI 231 x SLI 499 - $LaCl_3$	0.000385	SLI 231 x SLI 499 - $LaCl_3$	1
SLI 231 x SLI 505 - $LaCl_3$	0.1099	SLI 231 x SLI 505 - $LaCl_3$	1
SLI 231 x SLI 575 - $LaCl_3$	0.002493	SLI 231 x SLI 575 - $LaCl_3$	0.03123
SLI 233 x SLI 499 - $LaCl_3$	0.004892	SLI 233 x SLI 499 - $LaCl_3$	0.9737
SLI 233 x SLI 505 - $LaCl_3$	0.8575	SLI 233 x SLI 505 - $LaCl_3$	0.9763
SLI 233 x SLI 575 - $LaCl_3$	0.0807	SLI 233 x SLI 575 - $LaCl_3$	0.01756
SLI 499 x SLI 505 - $LaCl_3$	0.001474	SLI 499 x SLI 505 - $LaCl_3$	1
SLI 499 x SLI 575 - $LaCl_3$	0.1419	SLI 499 x SLI 575 - $LaCl_3$	0.03167
SLI 505 x SLI 575 - $LaCl_3$	0.02013	SLI 505 x SLI 575 - $LaCl_3$	0.01953
SLI 231 x SLI 233 + $LaCl_3$	0.003649	SLI 231 x SLI 233 + $LaCl_3$	0.5874
SLI 231 x SLI 499 + $LaCl_3$	0.05221	SLI 231 x SLI 499 + $LaCl_3$	0.9987
SLI 231 x SLI 505 + $LaCl_3$	1	SLI 231 x SLI 505 + $LaCl_3$	0.7883
SLI 231 x SLI 575 + $LaCl_3$	0.006383	0.SLI 231 x SLI 575 + $LaCl_3$	0.0005726
SLI 233 x SLI 499 + $LaCl_3$	0.1471	SLI 233 x SLI 499 + $LaCl_3$	0.4589
SLI 233 x SLI 505 + $LaCl_3$	0.002128	SLI 233 x SLI 505 + $LaCl_3$	0.98
SLI 233 x SLI 575 + $LaCl_3$	0.9563	SLI 233 x SLI 575 + $LaCl_3$	0.0002413
SLI 499 x SLI 505 + $LaCl_3$	0.03278	SLI 499 x SLI 505 + $LaCl_3$	0.6414
SLI 499 x SLI 575 + $LaCl_3$	0.3161	SLI 499 x SLI 575 + $LaCl_3$	0.0006731
SLI 505 x SLI 575 + $LaCl_3$	0.003754	SLI 505 x SLI 575 + $LaCl_3$	0.0001875

5 mM Vanillic Acid ± $LaCl_3$

Growth Rate		**Final Yield**	
Comparison	**p-value**	**Comparison**	**p-value**
SLI 231 ± $LaCl_3$	0.1459	SLI 231 ± $LaCl_3$	0.0005
SLI 233 ± $LaCl_3$	0.7953	SLI 233 ± $LaCl_3$	0.002389
SLI 499 ± $LaCl_3$	0.1194	SLI 499 ± $LaCl_3$	0.04408
SLI 505 ± $LaCl_3$	0.01286	SLI 505 ± $LaCl_3$	0.02268
SLI 575 ± $LaCl_3$	0.6059	SLI 575 ± $LaCl_3$	0.7737
sp. AMS5 ± $LaCl_3$	0.08744	sp. AMS5 ± $LaCl_3$	0.4056
SLI 231 x SLI 233 - $LaCl_3$	0.788	SLI 231 x SLI 233 - $LaCl_3$	1
SLI 231 x SLI 499 - $LaCl_3$	0.9988	SLI 231 x SLI 499 - $LaCl_3$	0.9978
SLI 231 x SLI 505 - $LaCl_3$	0.6593	SLI 231 x SLI 505 - $LaCl_3$	0.9547
SLI 231 x SLI 575 - $LaCl_3$	1	SLI 231 x SLI 575 - $LaCl_3$	0.000497
SLI 231 x sp. AMS5 - $LaCl_3$	0.001096	SLI 231 x sp. AMS5 - $LaCl_3$	0.02093
SLI 233 x SLI 499- $LaCl_3$	0.5811	SLI 233 x SLI 499- $LaCl_3$	0.9905
SLI 233 x SLI 505- $LaCl_3$	0.1241	SLI 233 x SLI 505- $LaCl_3$	0.9811
SLI 233 x SLI 575- $LaCl_3$	0.727	SLI 233 x SLI 575- $LaCl_3$	0.000395
SLI 233 x sp. AMS5 - $LaCl_3$	0.000169	SLI 233 x sp. AMS5 - $LaCl_3$	0.01604
SLI 499 x SLI 505- $LaCl_3$	0.8523	SLI 499 x SLI 505- $LaCl_3$	0.8003

SLI 499 x SLI 575 - $LaCl_3$	0.9998	SLI 499 x SLI 575 - $LaCl_3$	0.000938
SLI 499 x sp. AMS5- $LaCl_3$	0.001957	SLI 499 x sp. AMS5- $LaCl_3$	0.0428
SLI 505 x SLI 575 - $LaCl_3$	0.7242	SLI 505 x SLI 575 - $LaCl_3$	0.000151
SLI 505 x sp. AMS5 - $LaCl_3$	0.0128	SLI 505 x sp. AMS5 - $LaCl_3$	0.005178
SLI 575 x sp. AMS5- $LaCl_3$	0.001309	SLI 575 x sp. AMS5- $LaCl_3$	0.2517
SLI 231 x SLI 233 + $LaCl_3$	0.8618	SLI 231 x SLI 233 + $LaCl_3$	
SLI 231 x SLI 499 + $LaCl_3$	0.9976	SLI 231 x SLI 499 + $LaCl_3$	0.9983
SLI 231 x SLI 505 + $LaCl_3$	0.04592	SLI 231 x SLI 505 + $LaCl_3$	0.8716
SLI 231 x SLI 575 + $LaCl_3$	0.9691	SLI 231 x SLI 575 + $LaCl_3$	0.0002235
SLI 231 x sp. AMS5 + $LaCl_3$	3.07E-08	SLI 231 x sp. AMS5 + $LaCl_3$	4.54E-07
SLI 233 x SLI 499 + $LaCl_3$	0.6388	SLI 233 x SLI 499 + $LaCl_3$	0.000003121
SLI 233 x SLI 505 + $LaCl_3$	0.2714	SLI 233 x SLI 505 + $LaCl_3$	0.6685
SLI 233 x SLI 575+ $LaCl_3$	0.9989	SLI 233 x SLI 575+ $LaCl_3$	1.28E-04
SLI 233 x sp. AMS5 + $LaCl_3$	1.42E-08	SLI 233 x sp. AMS5 + $LaCl_3$	3.16E-07
SLI 499 x SLI 505 + $LaCl_3$	0.02222	SLI 499 x SLI 505 + $LaCl_3$	2.06E-06
SLI 499 x SLI 575 + $LaCl_3$	0.8327	SLI 499 x SLI 575 + $LaCl_3$	0.001131
SLI 499 x sp. AMS5 + $LaCl_3$	4.21E-08	SLI 499 x sp. AMS5 + $LaCl_3$	0.000001286
SLI 505 x SLI 575 + $LaCl_3$	0.1584	SLI 505 x SLI 575 + $LaCl_3$	0.00001043
SLI 505 x sp. AMS5 + $LaCl_3$	3.60E-09	SLI 505 x sp. AMS5 + $LaCl_3$	0.001483
SLI 575 x sp. AMS5 + $LaCl_3$	1.81E-08	SLI 575 x sp. AMS5 + $LaCl_3$	0.03846

SLI 575/*lanM* ± IPTG

Growth Rate in 20 mM MeOH		**Growth Rate in 34 mM EtOH**	
Comparison	**p-value**	**Comparison**	**p-value**
2 µM $LaCl_3$ ± IPTG	0.9924	2 µM $LaCl_3$ ± IPTG	0.2604
50 nM $LaCl_3$ ± IPTG	0.02077	50 nM $LaCl_3$ ± IPTG	0.00736
1 µM La_2O_3 ± IPTG	0.00772	1 µM La_2O_3 ± IPTG	0.000704
25 nM La_2O_3 ± IPTG	0.01731	25 nM La_2O_3 ± IPTG	0.09511